DEMONSTRATION REPORT

Dipole Discrimination Techniques Applied to Live Sites

MetalMapper Survey, Waikoloa HI

ESTCP Project MR-201226

NOVEMBER 2017

Leonard Pasion
Black Tusk Geophysics, Inc.

ESTCP

Page Intentionally Left Blank

Page Intentionally Left Blank

REPORT DOCUMENTATION PAGE	*Form Approved* *OMB No. 0704-0188*

1. REPORT DATE *(DD-MM-YYYY)*
11/30/2017

2. REPORT TYPE
ESTCP Demonstration Report

3. DATES COVERED *(From - To)*
9/29/2012 - 3/28/2018

4. TITLE AND SUBTITLE
Dipole Discrimination Techniques Applied to Live Sites

MetalMapper Survey, Waikoloa HI

5a. CONTRACT NUMBER
Contract: 12-C-0079

5b. GRANT NUMBER

5c. PROGRAM ELEMENT NUMBER

6. AUTHOR(S)
Leonard Pasion

5d. PROJECT NUMBER
MR-201226

5e. TASK NUMBER

5f. WORK UNIT NUMBER

7. PERFORMING ORGANIZATION NAME(S) AND ADDRESS(ES)
Black Tusk Geophysics, Inc.
2386 East Mall Suite 112A
Vancouver, BC
V6T 1Z3

8. PERFORMING ORGANIZATION REPORT NUMBER
MR-201226

9. SPONSORING/MONITORING AGENCY NAME(S) AND ADDRESS(ES)
Environmental Security Technology Certification Program
4800 Mark Center Drive, Suite 17D03
Alexandria, VA 22350-3605

10. SPONSOR/MONITOR'S ACRONYM(S)
ESTCP

11. SPONSOR/MONITOR'S REPORT NUMBER(S)
MR-201226

12. DISTRIBUTION/AVAILABILITY STATEMENT
Distribution A; unlimited public release

13. SUPPLEMENTARY NOTES

14. ABSTRACT
This Demonstration Report describes processing of cued MetalMapper collected as part of an ESTCP demonstration conducted at the former Waikoloa Maneuver Area, Hawaii. A spatially-variable magnetic soil response was observed at this site, and separation of soil and target response during inversion was required to obtain useful polarizabilities for classification. The research team modelled soil response using a two-object inversion approach: one dipole source was fixed at 0.9 m depth below the ground and fit a soil response characterized by a log-linear time decay. The second source fit the dipolar response of any metallic target present in the cued sounding.

15. SUBJECT TERMS
Advanced Geophysical Classification, Dipole Discrimination Techniques, Live Sites, MetalMapper Survey, Unexploded Ordnance

16. SECURITY CLASSIFICATION OF: a. REPORT	b. ABSTRACT	c. THIS PAGE	17. LIMITATION OF ABSTRACT	18. NUMBER OF PAGES	19a. NAME OF RESPONSIBLE PERSON
					Leonard Pasion
					19b. TELEPHONE NUMBER *(Include area code)*
UNCLASS	UNCLASS	UNCLASS	UNCLASS	56	604-428-3382

Page Intentionally Left Blank

Executive Summary

This Demonstration Report describes processing of cued MetalMapper collected as part of an ESTCP demonstration conducted at the former Waikoloa Maneuver Area, Hawaii.

A spatially-variable magnetic soil response was observed at this site, and separation of soil and target response during inversion was required to obtain useful polarizabilities for classification. We modelled soil response using a two-object inversion approach: one dipole source was fixed at 0.9 m depth below the ground and fit a soil response characterized by a log-linear time decay. The second source fit the dipolar response of any metallic target present in the cued sounding. Compared with our usual background subtraction approach for cued data, this processing strategy yielded a better match to library polarizabilities for likely targets of interest (TOI). Conventional background subtraction did not work in this case because spatial sampling of backgrounds was not sufficient to characterize the variability of soil response across the site.

Training data were selected using cluster analysis and comparison with a comprehensive polarizability library. We employed a two-stage classifier for the Waikoloa cued MetalMapper data. The first stage matched all three estimated polarizabilities for each model with our reference library. The second stage ranked targets based on model misfit with the estimated soil response, i.e. we prioritized targets with polarizabilities that were dissimilar to magnetic soil.

This classification diglist yielded nine missed QC seeds. Although two of the seeds could have been identified by matching with the primary polarizability, the data for the remaining seven seeds showed only a soil response and these targets were not therefore not detected in the cued data. Based on this result, we flagged all 939 cued targets for digging in our final diglist submission.

Retrospective analysis identified an additional seven TOI late in the diglist. Again, two of these likely false negatives could potentially be identified by matching with the primary polarizability. The remainder of the false negatives exhibited soil response only. We conclude that not all TOI were detectable with the MetalMapper at this site. Advanced processing can minimize soil effects but cannot eliminate them in all cases.

Table of Contents

List of Figures

List of Tables

Acronyms

AGC	Advanced Geophysical Classification
BTG	Black Tusk Geophysics
cm	Centimeter
CSV	Comma Separated Variable
DAGCAP	DoD Advanced Geophysical Classification Accreditation Program
ESTCP	Environmental Security Technology Certification Program
HI	Hawaii
IVS	Instrument Verification Strip
m	Meter
mm	Millimeter
ms	Millisecond
MM	MetalMapper
MPV	Man Portable Vector
QC	Quality Control
ROC	Receiver Operating Characteristic
s	Second
SERDP	Strategic Environmental Research and Development Program
SOI	Single Object Inversion
2OI	Two Object Inversion
3OI	Three Object Inversion
TOI	Target of Interest
UXO	Unexploded Ordnance
WMA	Waikoloa Maneuver Area

1 Introduction

The former Waikoloa Maneuver Area (WMA) is located on the Big Island of Hawaii and was used by the Navy as a training and artillery range during World War II. In 2013 an ESTCP demonstration was carried out at WMA in grids selected from areas of interest at the site. Suspected munitions present at the demonstration site included:

- 60-mm and 80-mm high explosive mortars
- 75-mm, 105-mm, and 155-mm projectiles
- 2.36-inch rocket propelled anti-tank rounds
- US MK II hand grenades
- Rockets
- M1 anti-tank land mines
- Japanese ordnance

This Demonstration Report summarizes processing carried out by Black Tusk Geophysics on cued MetalMapper data acquired at WMA.

2 Technology description

2.1 MetalMapper electromagnetic induction sensor

The MetalMapper (Figure 1) is a next generation electromagnetic induction (EMI) sensor designed for classification of buried unexploded ordnance (UXO). Three orthogonal transmitter coils provide diverse excitation of buried conductive targets. Seven receiver “cubes” each measure orthogonal components of the induced secondary magnetic field.

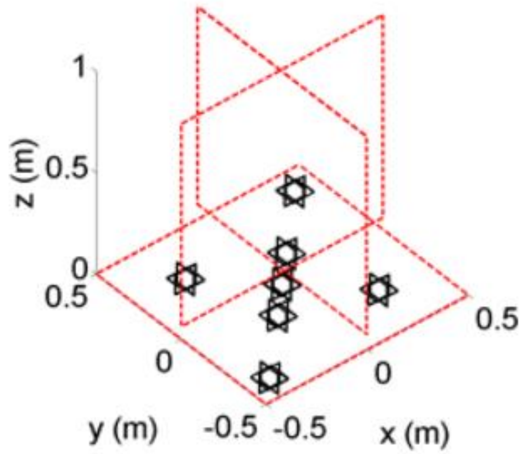

Figure 1. MetalMapper sensor geometry. Red dashed lines indicate transmitter coils and solid black lines are receiver cubes.

The MetalMapper can be deployed for detection surveys that map metallic targets at a site. In this study, the sensor was used for cued interrogations where the array was positioned over targets identified in a previous detection survey and EMI data were collected for classification.

2.2 Classification

Classification with EMI data uses inversion to fit observed EMI data collected over each target. The forward model is typically parameterized by the target location, orientation and dipole polarizabilities. The polarizabilities provide information about intrinsic target properties including size, shape and material composition. Advanced geophysical classification (AGC) relies on matching estimated polarizabilities with a predefined library to identify likely targets of interest (TOI).

Classification processing can be complicated by the presence of a strong background soil response that is superimposed on conductive target response. Hawaiian soils can be strongly ferromagnetic, and the relaxation of magnetic domains after application of a primary magnetic field produces a characteristic log-linear response in observed time-domain EMI data. Separating the soil and target responses in MetalMapper cued data was one of the primary challenges for this classification study.

3 Cued MetalMapper Processing

3.1 Feature extraction

The Waikoloa Maneuver Area MetalMapper cued dataset comprised 939 anomalies collected in three distinct areas (Figure 2).

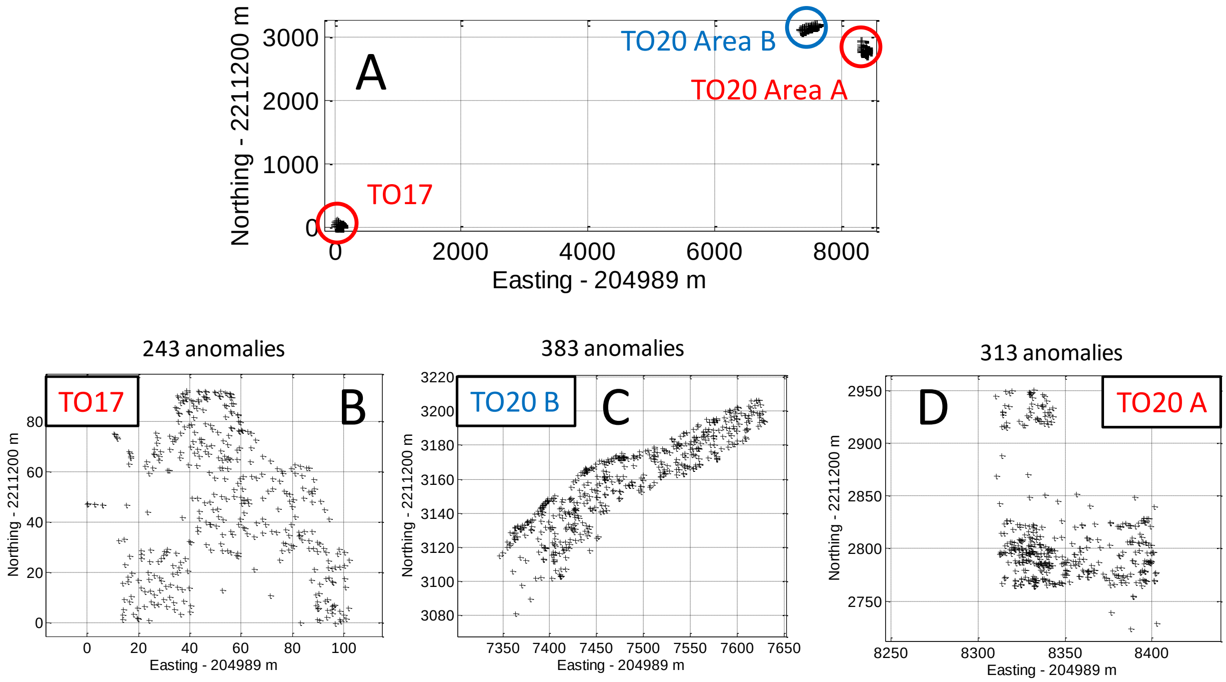

Figure 2. Location of MetalMapper cued anomaly acquisitions (small + symbols). (A) Relative location of the three different acquisition areas. (B-D) Close-up maps of the anomaly acquisition locations for each area.

Preliminary inspection of the data and inversion results suggested that many of the anomalies are "soil anomalies", i.e., the EM61 anomaly picks arose from geology (magnetic soil) rather than metallic objects in the ground. MetalMapper data for this type of anomaly has a recognizable appearance in which the decay of the components that are sensitive to magnetic soil is linear (in log-log space) with an exponential decay rate of about 1.3. We developed a soil model from MetalMapper soundings that look like pure soil response (Figure 3). As described below, this was used during data QC to aid in the identification of soil anomalies. In addition we found that the soil component of the data can frequently be fit well with a large, deep, plate-like target centered on the MetalMapper array. We used this discovery as described below.

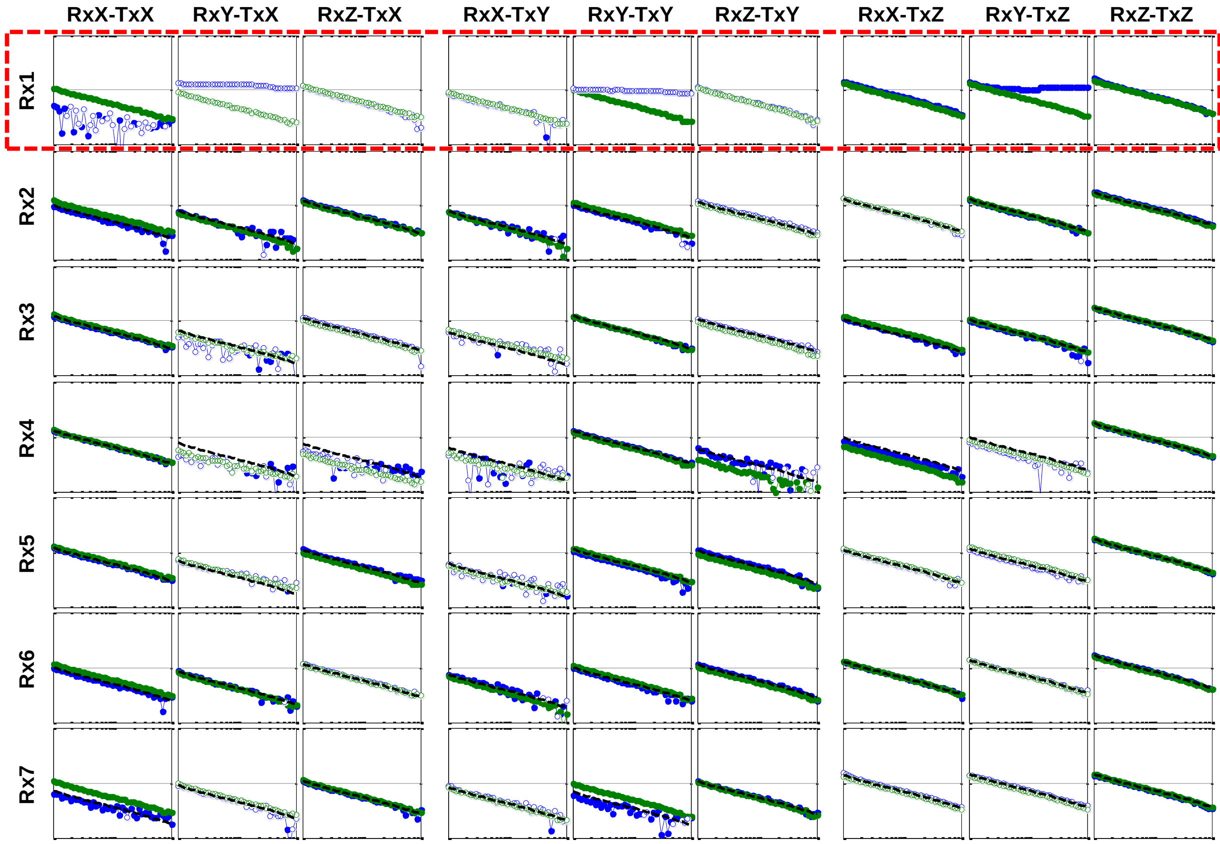

Figure 3. Typical data for a soil anomaly (Anomaly 628 – Area 20A). Blue dots/lines are observed data; green dots/lines are predicted data. Broken black line on top of the predicted and observed data represents typical decay for a pure soil response. In this case the black line generally falls directly on top of the observed data for most components. Note that receiver 1 (Rx1; top row) was not functioning for all data acquired at Waikoloa; these data were omitted during inversions.

MetalMapper cued data for all anomalies were received as a set of raw CSV files for both the cued anomaly data and the background measurements. For this project two types of background measurements were collected at each background location:

1. an "in-air" background with the sensor array elevated;
2. a "normal" background with the sensor array on the ground.

All CSV files were imported into UXOLab. The data were inverted in UXOLab using a sequential inversion approach to estimate target location, depth and primary polarizabilities. Instrument height above the ground was assumed to be 14 cm. Noise standard deviation estimates were not available, so a constant noise value of 1 over all time channels was used. Target location was constrained to lie between ±0.7 m in both X and Y directions relative to the acquisition location. Target depth was constrained to lie between –1.2 and 0 m. The initial optimization for target location identified up to eight starting models to input into the subsequent estimation of polarizabilities.

We performed six inversions per anomaly, comprising two sets of three inversions. In both sets we solved for (1) a single object (single object inversion: SOI); (2) two objects (2OI); and (3) three objects (3OI), resulting in six models per anomaly. In the first set we used data that were background corrected using the nearest in-air background measurement. For the two- and three-object inversions, the location of one source was fixed at the center of the MetalMapper array at a depth of 90 cm. The fixed source is intended to represent the soil component of the signal. The single-object inversion in this set is typically unreliable because not all background signal has been removed (Figure 4).

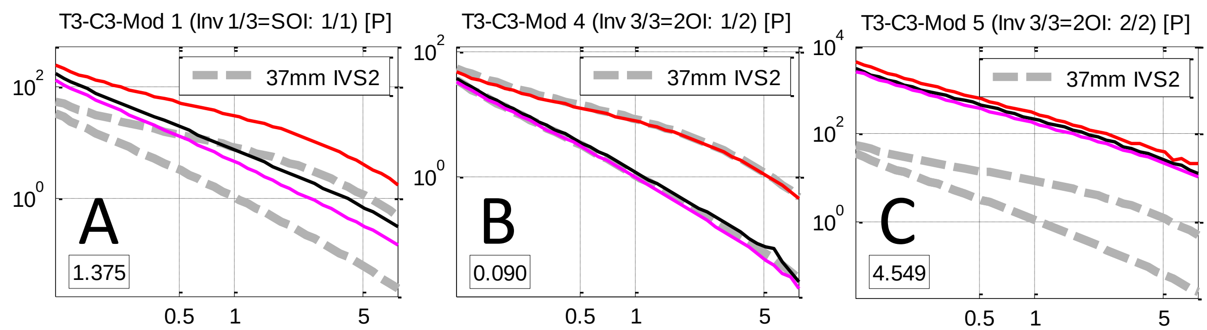

Figure 4. Example inversion results for a 37mm projectile in the IVS using an in-air background measurement for background correction, and fixing one source at 90 cm depth for the 2OI. (A) Single object inversion result: amplitude of recovered polarizabilities is much too high because the data contain a large background signal due to geology. (B-C) Two object-inversion results: the source depth for model C was fixed at 90 cm. The recovered polarizabilities are typical of a pure soil response. The other model (B) accurately recovers the polarizabilities of the 37mm projectile. Colored lines are predicted polarizabilities. Broken grey lines are 37mm reference polarizabilities.

In the second set of inversions we used data that were corrected using the nearest "normal" background measurement (i.e. collected with the sensor array on the ground). No source locations were fixed. With a background measurement representative of the background response at the anomaly location, this second approach can work well. Unfortunately, for the Waikoloa dataset the spatial variation in background response is large and the spatial coverage of the background measurements is poor (particularly for areas TO17 and TO20A; Figure 5). As a result, frequently either too much or not enough background is subtracted, leading to poor, unreliable inversion results. An example comparison of the results obtained using this approach versus the in-air background/fixed source approach is shown in Figure 6.

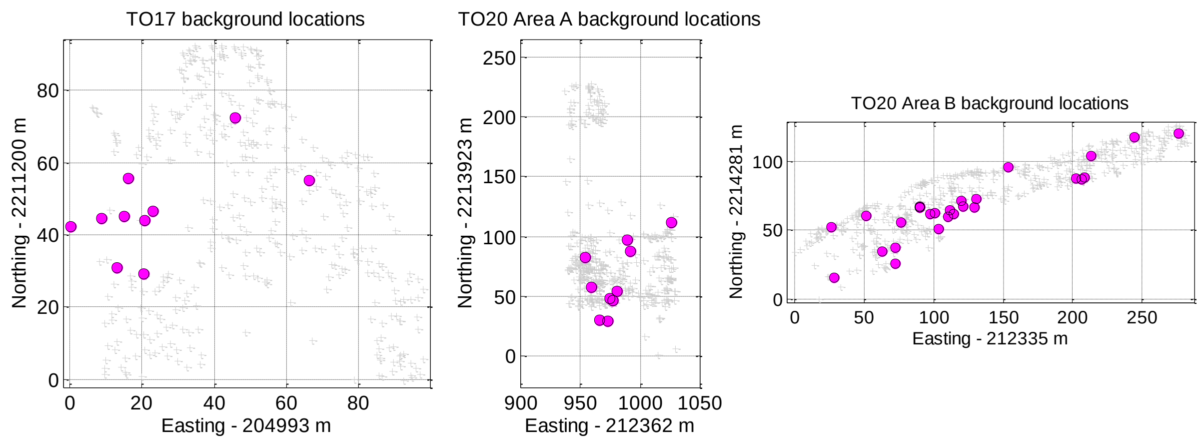

Figure 5. Background measurement locations for the three areas (magenta dots). Note the relatively small number of locations and poor spatial coverage, particularly for areas TO17 and TO20A.

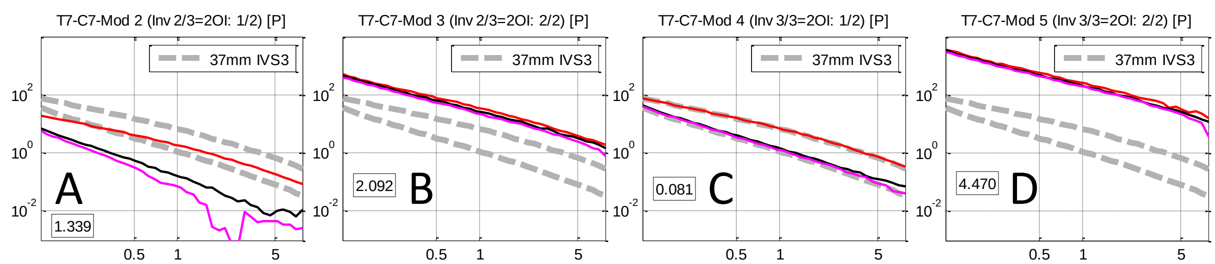

Figure 6. Comparison of 2 object inversion results using normal (near-ground) background measurement for background correction (A-B), and in-air background measurement with one fixed source (model D) at 90 cm depth (C-D). In this example (37mm, IVS measurement) the result using the in-air background-corrected data with one fixed source is clearly superior (compare model C versus model A).

Analysis of the data, including visual QC of data and model parameters, selection of training data, and dig list creation, was performed using the UXOLab software suite. Visual QC of the data was performed using the UXOLab module *QCZilla*, which provides a thorough overview of the observed and predicted data, predicted model parameters, and measures of data/model quality. Display of the gridded EM61 data at each anomaly provides a useful indicator of the anomaly size and strength. Predicted polarizabilities were compared to reference polarizabilities for various ordnance items initially derived from IVS and test pit measurements. The Waikoloa IVS contained two types of 37mm projectiles; the test pit contained 37mm, 60mm, and an 81mm mortar, with measurements taken at various depths and orientations. As the analysis proceeded, the library of reference items was augmented with additional items based on a comparison of the predicted polarizabilities with polarizabilities for known TOI from various past Live Site demonstrations. Ground truth obtained through training data requests and partial ground truth was also used to augment the ordnance reference library used for classification. Each item in the ordnance reference library was assigned a size (diameter) in mm. Each item with a dig decision of "dig" in the submitted dig list was assigned a size category (1 for diameter <50mm; 2 for 50≤diameter≤100mm; and 3 for diameter>100mm) based on the ordnance item in the reference library with the best matching primary polarizability (L1).

During data/model QC the primary objectives were to (1) flag high-likelihood TOI anomalies; (2) flag anomalies to be requested as training data; (3) fail bad models and inversions; and (4) identify likely soil anomalies. Anomalies flagged as high-likelihood TOI were monitored during the dig list creation phase to ensure they were being dug, ideally early in the dig list. Models and inversions were considered to be bad when the inversion failed (i.e., the data misfits are large), or when the recovered model location(s) were on, or near, an inversion boundary. Bad models and inversions were identified in a semi-automated manner. E.g., models would be sorted by different measures of model/data quality and the visual QC process would focus on the models with the poorest quality. Using our Waikoloa soil model, we calculated the misfit between the soil model and the observed data for each anomaly. A single scale factor was calculated for each anomaly such that the misfit was minimized. Low misfit values (e.g., <0.6) are indicative of a high likelihood soil anomaly. We used this during QC to help automatically identify soil anomalies. Figure 7 shows the variability in soil misfit for the three different areas. In TO20 Area A most of the anomalies have a low soil misfit suggesting most of the anomalies arise from magnetic soil. The mean soil misfit is largest for TO20 Area B, suggesting classification may be easier in this area due to weaker magnetic soil effects. Figure 3 shows data for a typical soil anomaly; soil misfit for this anomaly is 0.43. Polarizabilities for this anomaly are shown in Figure 8.

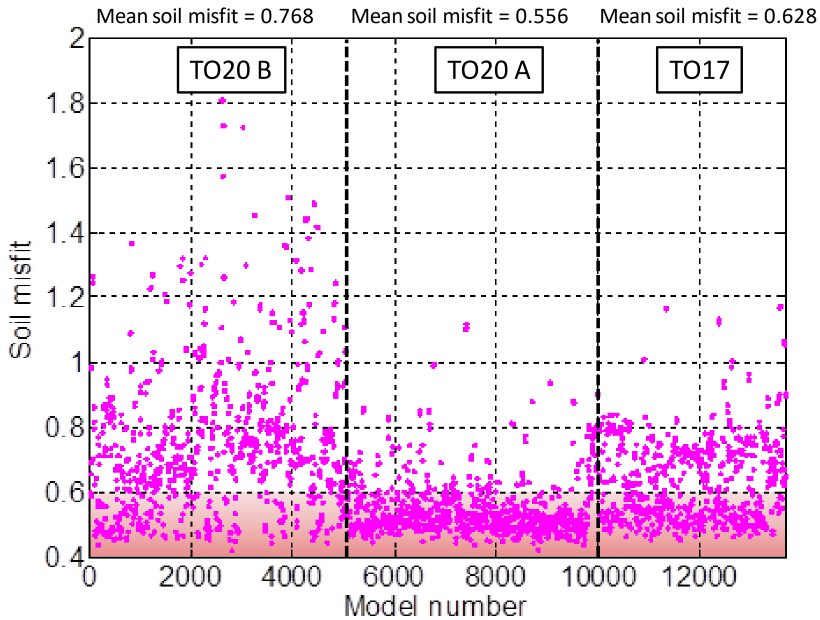

Figure 7. Soil model misfits for the Waikoloa MetalMapper cued dataset. Mean soil misfit values shown at the top are a measure of the deviation between the observed data and data representative of a pure "soil" anomaly. Soil misfit values less than ~0.6 (red-shaded region) are typically indicative of a very strong soil response. Mean soil misfit is lowest for area TO20A suggesting that the soil response here is strongest and many of the anomalies will be due solely to magnetic soil.

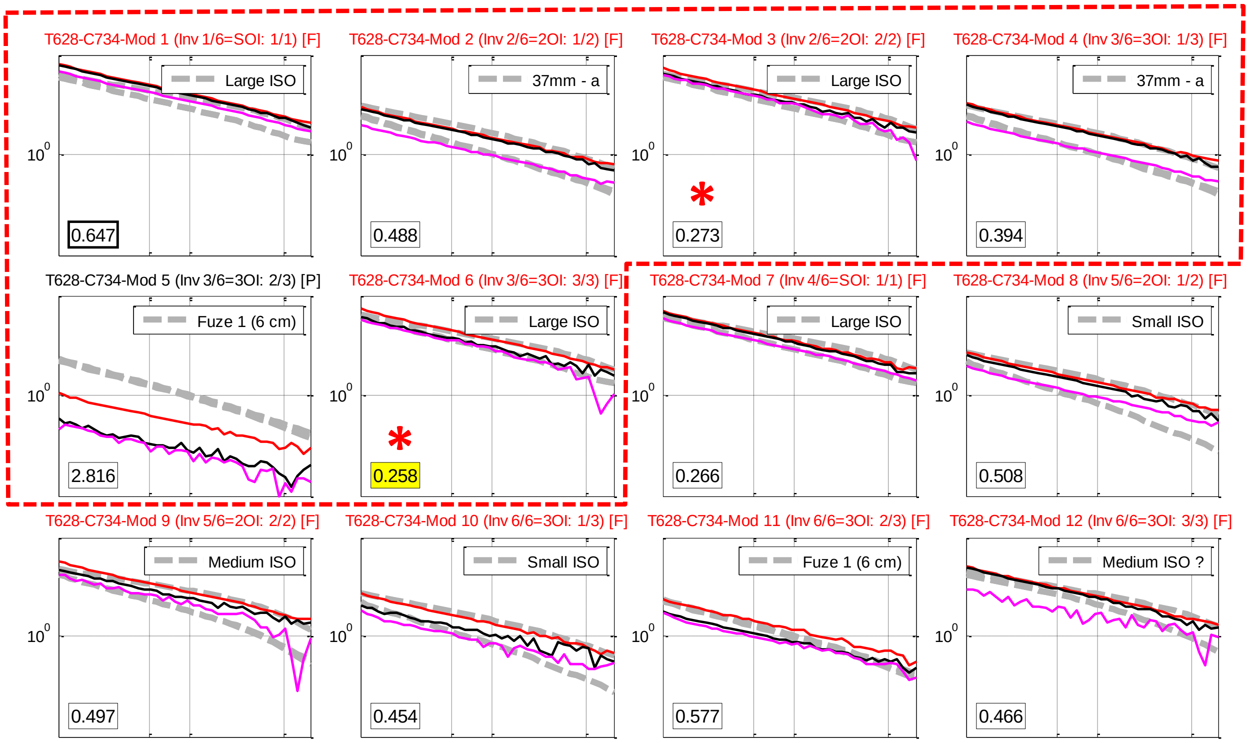

Figure 8. Polarizabilities for a soil anomaly (Anomaly 628; area TO20A). First six models (red outline) are SOI, 2OI and 3OI results using in-air background measurement for background correction and, for 2OI and 3OI, fixing one source at 90 cm depth (red asterisk). Remaining models used the nearest near-ground background measurement for background correction. Polarizabilities for a soil anomaly typically have a linear decay (in log-log space) and a relatively high degree of jitter. Models representing soil typically are high amplitude and have three near-equal amplitude polarizabilities. Other models, which are primarily artifacts from the multi-object inversion process, typically are small and frequently have equal primary and secondary polarizabilities.

With multi-object inversions it is not uncommon that one of the models is unrealistic (e.g., deep, large in magnitude, sometimes located on or near a horizontal inversion boundary) yet provides the best fit to the reference polarizabilities. In all of these cases the model was flagged as failed. Models flagged as failed were not used in the classification process. Anomalies with all models from all inversions failed were classified as “cannot extract reliable parameters”; these anomalies were dug. For a given anomaly, if more than one model was passed the classification procedure will consider all passed models and use the one that is “best” - based on the classification metric - for the dig decision.

The Waikoloa MetalMapper Cued dataset comprised 939 unique anomalies. Of the 13692 total models, 6288 were passed and used in the classification process; 7404 were failed. No anomalies were classified as “cannot extract reliable parameters.” 187 anomalies were classified as “high likelihood UXO” during QC; 81 of these (43%) correspond to actual TOI. The total number of unique TOI in the MetalMapper Cued dataset is 98.

3.2 Classification

3.2.1 Training data selection

Figure 9 shows the distribution of models in decay versus size feature space. The overlap between some of the test pit reference features with regions of high feature density suggest that classification may be difficult because a relatively large proportion of scrap and/or geology-based models will look similar to TOI.

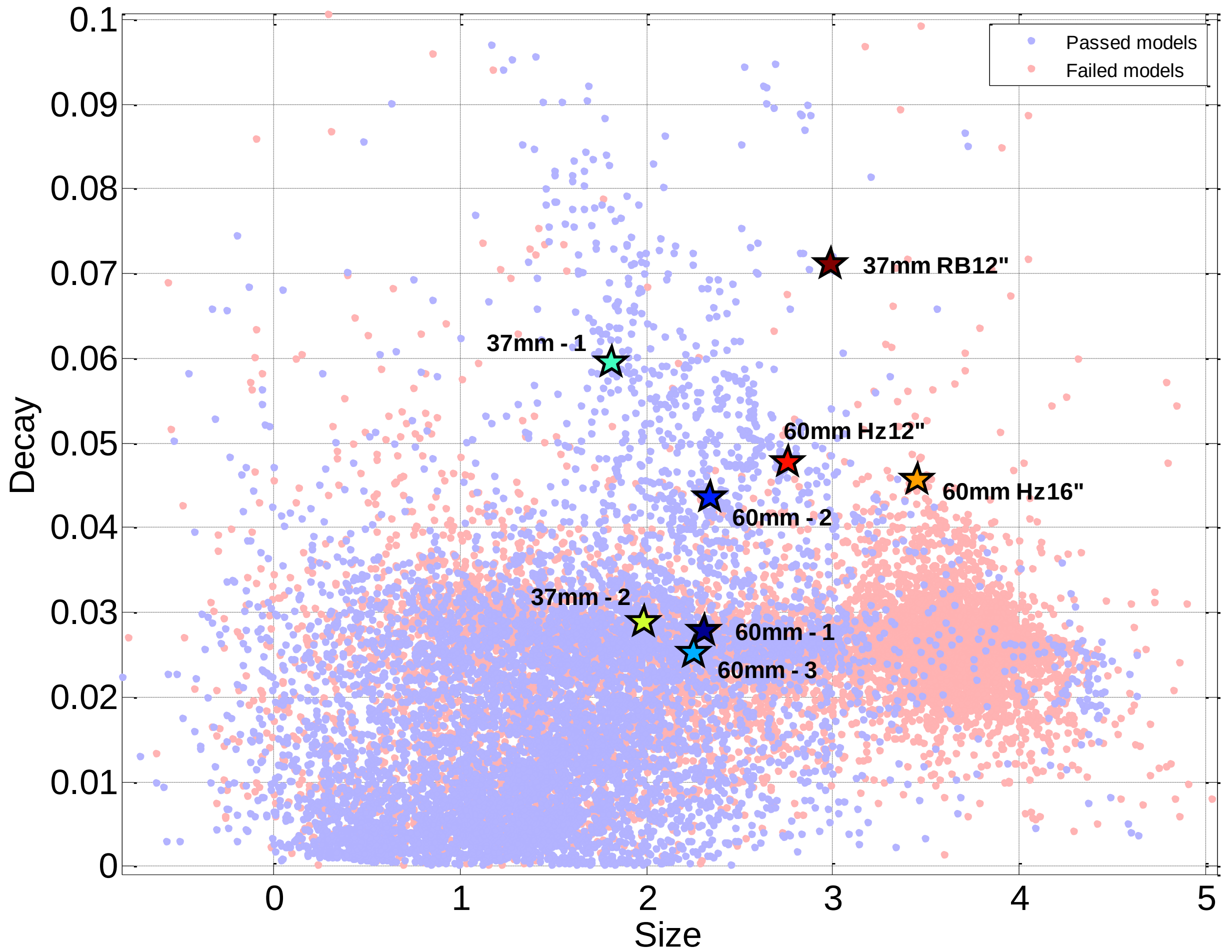

Figure 9. Distribution of models in decay(t1,t29) versus size(t1) feature space, where size(t1) is the total polarizability measured at the first time channel (t1=0.106 ms), and decay(t1,t29) is size(t1)/size(t29) where t29=2.006 ms. A few outliers are not shown. Labeled stars represent ordnance library reference items based on test pit measurements. Failed models were not used in the classification process.

Our analysis method is based on polarizability matching with respect to ordnance items in a reference library. For this approach to be successful it is important to determine the types of ordnance present at the site. During visual QC the analyst keeps track of suspicious, UXO-like items (i.e., items with modeled polarizabilities possessing UXO-like properties). Training data for some of these, particularly those with polarizabilities different from the items in the current reference library, would be requested. In addition, we used our custom training data selection tool, *TrainZilla*, to explore feature space and automatically search for clusters of items with self-similar polarizabilities. In *TrainZilla*, the user selects a region in feature space by drawing a polygon, and the program automatically identify clusters of self-similar feature vectors by computing a misfit matrix **M** with elements

$$M_{jk} = \sum_{i=1}^{N} (L^{j}{}_{total}(t_i) - L^{k}{}_{total}(t_i))^2$$

where L^j_{total} is the log-transformed total polarizability for the j^{th} feature vector. Feature vectors with mutual misfit less than a user-specified threshold define a cluster in polarizability space. This analysis helps to identify clusters that may not be readily evident in decay-size feature space: e.g., targets with consistent polarizabilities that may be hidden in the "cloud" of non-TOI features. A basic example of the use of *TrainZilla* is shown in Figure 10 and Figure 11.

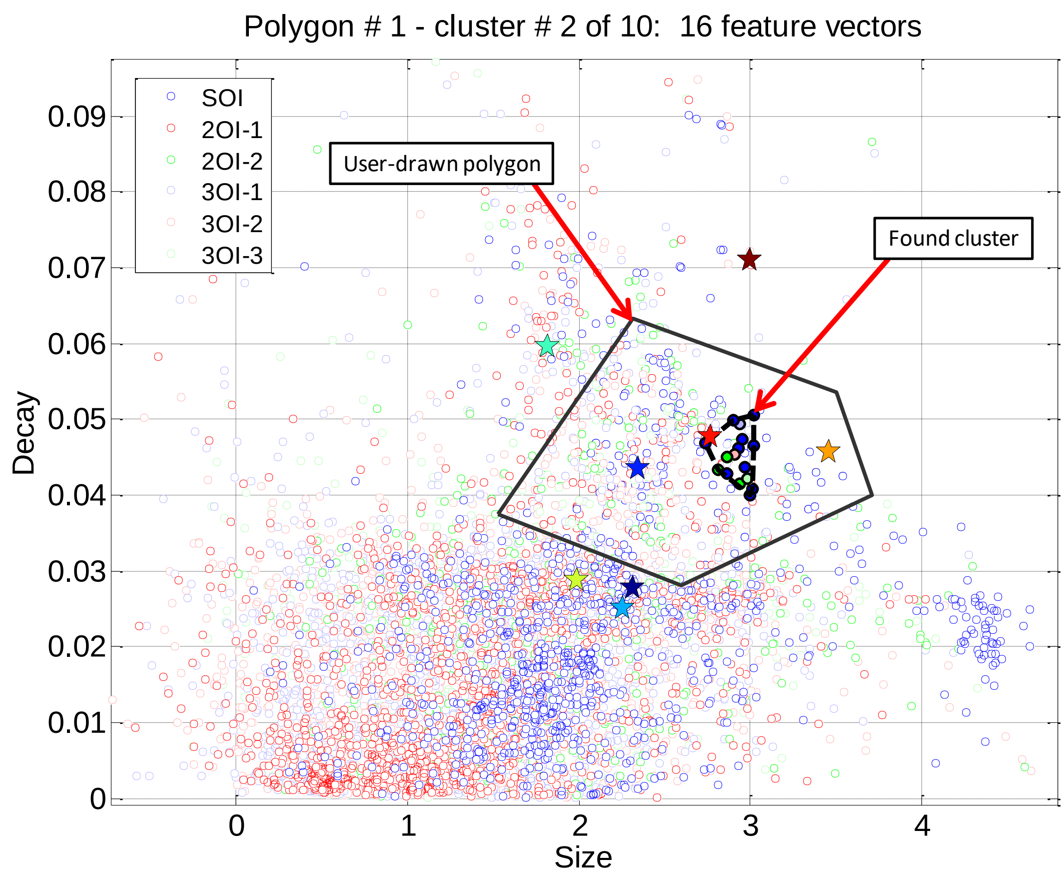

Figure 10. Example of use of the training data selection tool (*TrainZilla*). A polygon (solid black line) is drawn in feature space. Clusters of items with self-similar polarizabilities are automatically found based on the specified cluster search parameters. In this case a cluster comprising 10 features is visible (solid feature symbols encompassed by broken line). Polarizabilities for some of the models in this cluster are shown in Figure 11.

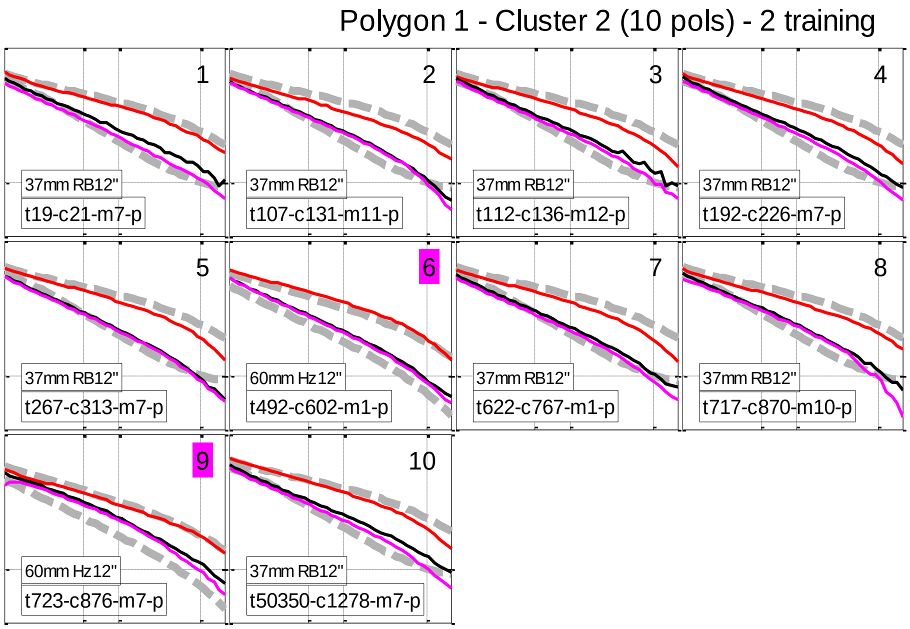

Figure 11. Polarizabilities for some of the models in the cluster shown in Figure 10. Colored lines are predicted polarizabilities. Broken grey lines are best fitting test pit reference polarizabilities. Training data were requested for two items (magenta highlighted index number). These were revealed to be a medium ISO (anomaly WK-492) and an 81mm mortar (anomaly WK-723).

Our training data requests typically focused on: (1) items whose polarizabilities exhibited UXO-like properties distinct from those of items in our reference library; (2) items with polarizabilities similar to items in our reference library, but with degraded quality (helpful for determining thresholds for polarizability matching); and (3) one-off items.

An alternative approach to selecting training data, geared primarily to finding potential one-off items, is to look for items with polarizabilities that closely match items in a large ordnance library. We do this with the UXOLab module called the *Ordnance Museum* (Figure 12), which comprises (for MetalMapper cued data) polarizabilities for more than 400 items (ranging in size from 20mm to 155mm) from past ESTCP live site demonstrations and other classification projects; 240 of these come from the UX-Analyze MetalMapper Cued polarization library. With the *Ordnance Museum* we can easily search for models in our dataset with similar polarizabilities to any of the museum items. For Waikoloa we found several items with close matches (polarizability misfit < 0.3 calculated using all three polarizabilities) to *Ordnance Museum* items. Six representative items, for which training data were requested, are shown in Figure 13.

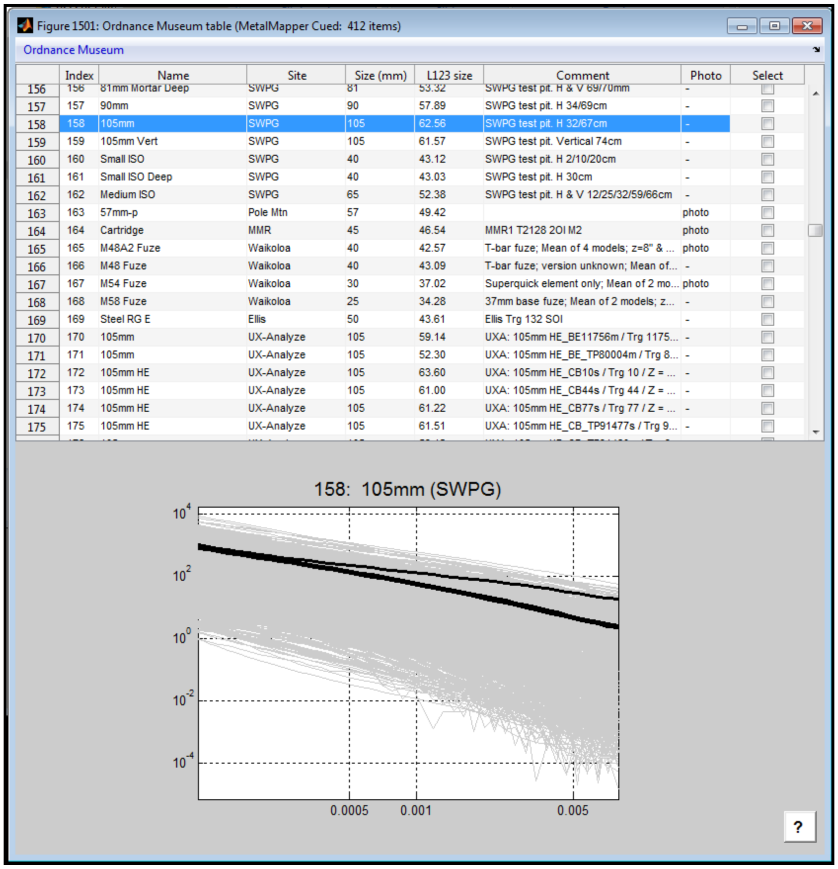

Figure 12. UXOLab *Ordnance Museum* interface. This is a large library of reference polarizabilities compiled from several ESTCP live site demonstrations, and other projects. The *Ordnance Museum* for MetalMapper cued data currently comprises approximately more than 400 items ranging in size from 20mm to 155mm projectiles.

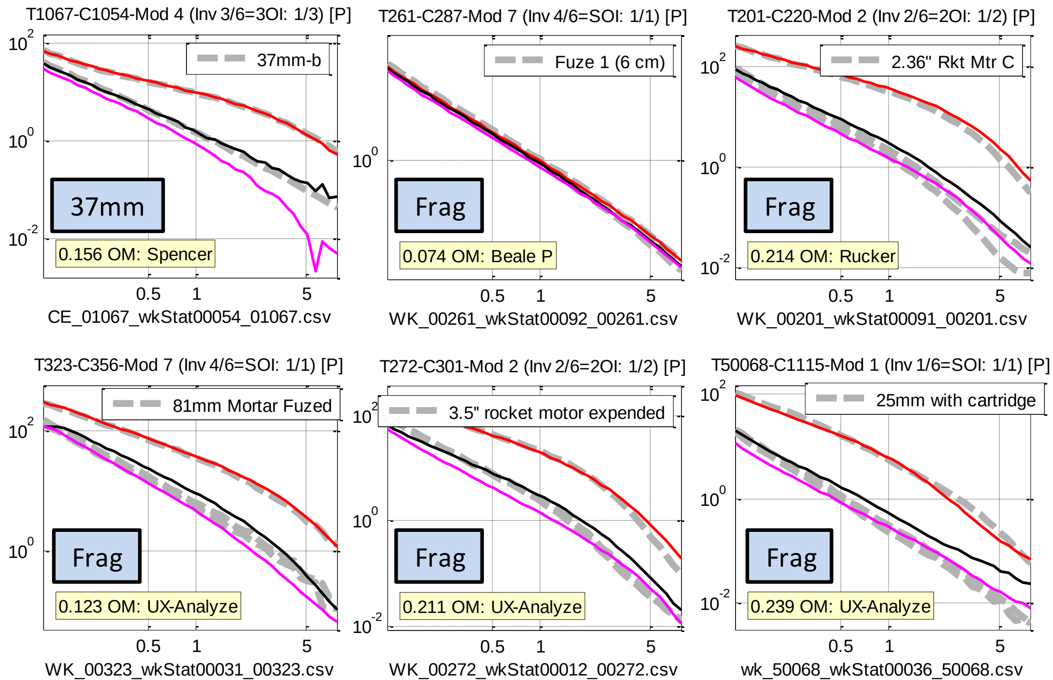

Figure 13. Example polarizabilities of models with close matches (misfit < 0.3 calculated using all three polarizabilities) to items in the *Ordnance Museum*. Anomaly labels are the number following the "T" in each plot title. Label at top right of each plot is best-fitting ordnance name. Labels in yellow boxes show the polarizability misfit and the source of the reference polarizabilities. Labels in blue show ground truth identification obtained in the training data request.

A single training request for 33 items was submitted. Of these, seven were TOI: 37mm (2), medium ISO, 60mm mortar, 81mm mortar (3). One item (WK-261) appears from the ground truth photo to be a fuze, but it was classified as frag). Based on these results, several classes of TOI were removed from our reference library: fuze, 105mm, hand grenade, small ISO (schedule 40), rocket motors.

3.2.2 Classification method

Our dig lists were developed using our visual classification software *DigZilla* (Figure 14), which is fully integrated with other elements of the UXOLab software suite. *DigZilla* allows for the creation of multi-stage dig lists with minimal effort, and supports a number of classifiers.

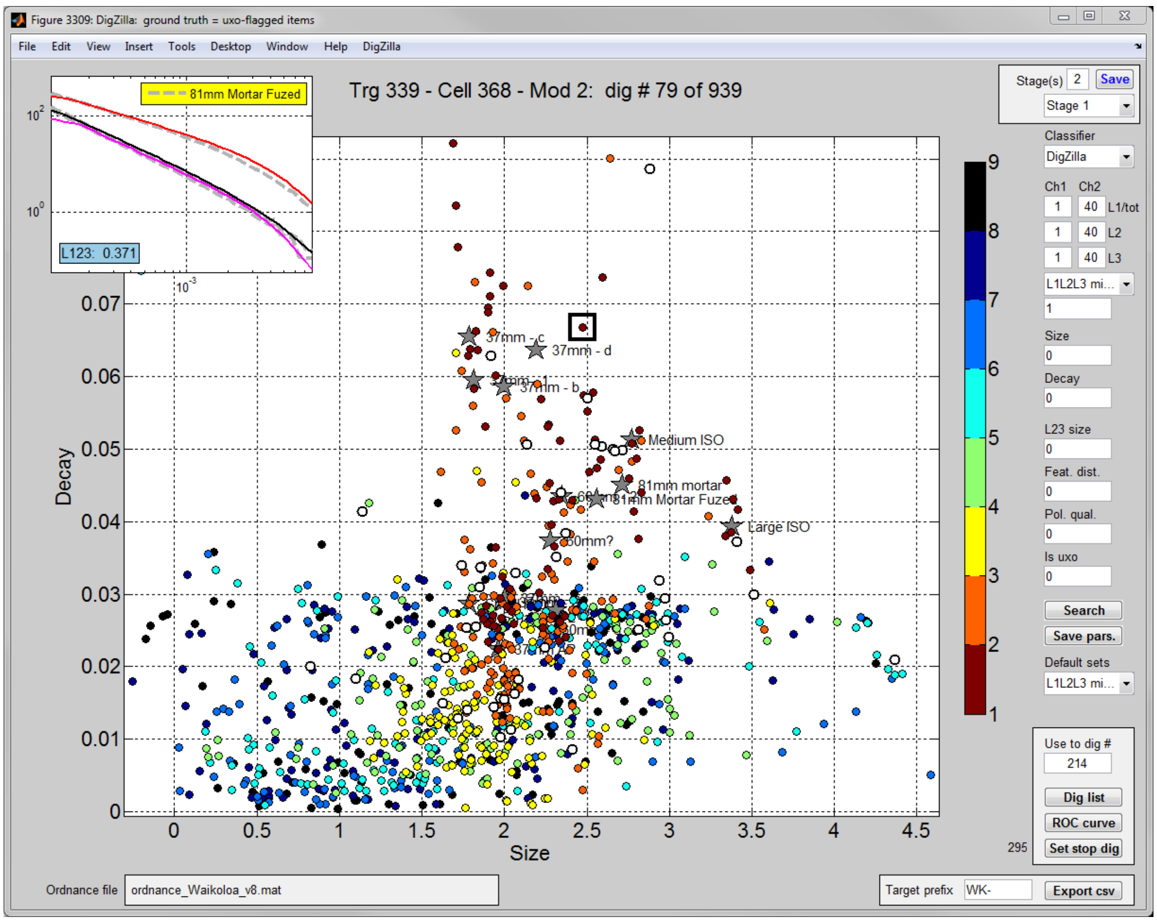

Figure 14. Screen shot of the UXOLab *DigZilla* graphical user interface. Features in the decay versus size feature plot are color coded according to dig list order. Stars are reference features.

Our stage 1 dig list comprised two parts. For part 1 (digs 1—214) classification was based on polarizability matching against a reference library using all three polarizabilities and the first 40 time channels (up to 6.41 ms). Figure 15 shows the items in the ordnance library used for part 1 of the dig list. For part 2 (digs 215—939), classification was based on the data misfit with our Waikoloa soil model. For the latter, anomalies with data closely resembling the soil model appear later on the dig list. The soil model misfit is calculated using an arbitrary scale factor for each anomaly to account for amplitude variations associated with the varying strength of the magnetic soil response across the site. The transition point between the two parts of the dig list was chosen by visual inspection of the polarizabilities in dig list order, with the transition point positioned just ahead of the point where polarizabilities sorted by matching against the reference library returned a majority of soil anomalies. Anomalies near the beginning of the second part of the dig list should represent anomalies with a substantial presence of metal in the ground, though their match to items in the reference library will not necessarily be good. This was considered to be a conservative approach for ensuring non-soil anomalies occur ahead of soil anomalies. The stop dig point for the stage 1 dig list was dig number 295.

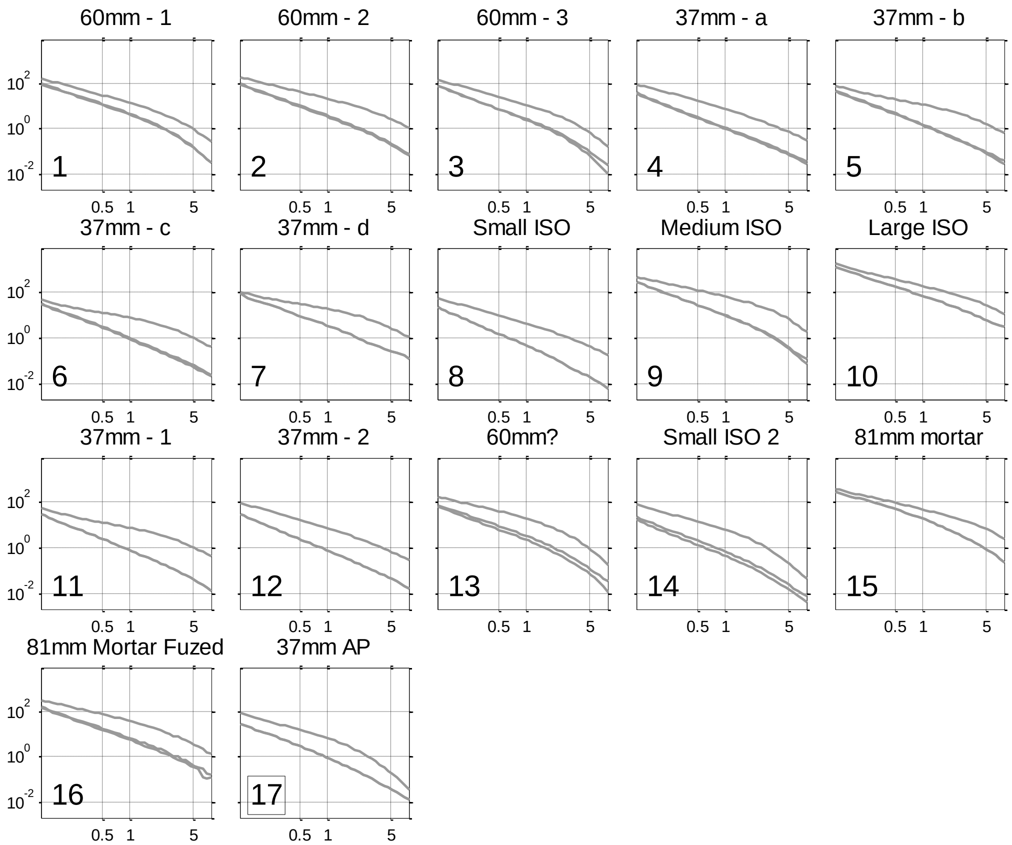

Figure 15. Items in the ordnance reference library used for part 1 of the stage 1 dig list.

Our stage 1 dig list missed nine QC seeds. Because of this we were required to submit a Failure Analysis Memo. An edited version of the Failure Memo, with repetitious material removed, is presented below.

Failure Analysis Memo

Site: Waikoloa
Analyst: Black Tusk Geophysics
Data: MM Cued
Date: January 23, 2015

Our stage 1 dig list missed nine QC seeds (see table below).

Table 1: List of nine missed QC seeds. Last column is a classification based on data match to a soil model and visual inspection of observed data and predicted polarizabilities.

Dig number	Anomaly	Survey Area	Identification	Depth (cm)	Soil anomaly?
370	402	TO20-A	37mm (TP)	29	No
383	1026	TO17	60mm Mortar	34	Yes
396	715	TO20-A	37mm	25	No
427	203	TO20-B	60mm	40	Yes
528	391	TO20-B	60mm mortar	45	Yes
555	393	TO20-B	60mm mortar	45	Yes
568	707	TO20-A	37mm	20	Yes
660	474	TO20-A	60mm mortar	40	Yes
692	73	TO20-B	37mm TP	11	Yes

The missed QC seeds were distributed amongst all three areas. The stop dig point on our stage 1 dig list was dig number 295. The missed QC seeds occurred between digs number 370 to 692. (Total number of anomalies is 939.)

a. Analysis of the factors that resulted in the misclassification of each missed seed

As described above, we used a two-pronged inversion approach (one set of inversions used in-air background-corrected data with a fixed source to represent the soil response; the other set used data corrected using near-ground background measurements), which results in a total of twelve models per anomaly. We believed this would provide the best chance of obtaining at least one good, representative model per anomaly.

Of the nine QC seeds we missed, only two (WK-402 and WK-715) were missed because their polarizability misfit was too large relative to the decision point we chose. For the other seven missed QC seeds, the data and polarizabilities are consistent with what we consider to be a typical soil response. For one of these seven (WK-73; 37mm

TP at 11 cm depth; Figure 16), the offset between ground truth location and MetalMapper acquisition location is large (74 cm). This likely explains the soil response at this anomaly.

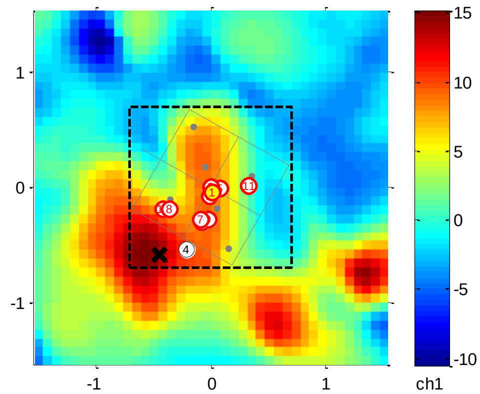

Figure 16. EM-61 data in the vicinity of WK-73 (37mm TP at 11 cm depth). Thin lines show outline of the MetalMapper. Broken black lines are horizontal inversion boundary. Circles are predicted model locations. Black "X" is ground truth location of the seed. Offset to center of the MetalMapper is about 74 cm.

b. Description of how the analysis procedures have been modified based on the additional information provided

QC seeds are typically missed because either (1) the polarizability match to reference items is somewhat worse than expected based on an assessment of overall data quality; or (2) the seed is a "one-off" item not discovered during training, and therefore not represented in the polarizability reference item. The corrective measure to take in both cases is obvious: either (1) modify the decision point so that items with larger polarizability misfits appear before the stop dig point; or (2) add the new item to the polarizability reference library. For this dataset, however, the key issue with most of the missed QC seeds is that the data contain no obvious signal beyond a soil response, resulting in recovered polarizabilities that bear no resemblance to those of the associated library item(s). This is exemplified by anomaly WK-707 (37mm ATP at 20 cm depth; Figure 17 and Figure 18). The similarity between the observed data and the soil model resulted in this anomaly appearing at dig number 568. There was no possibility that this anomaly would be dug early. A similar situation exists with WK-203, 391, 393, 474 and 1026 (See the Failure Memo Appendix for data and polarizabilities of these anomalies). Figure 19 shows polarizabilities for digs 541-576 and illustrates the difficulty in recognizing two of the missed QC seeds (WK-393 and WK-707) whose polarizabilities look very much like those from other soil anomalies. For this site, with several QC seeds that cannot be detected due to a very strong soil response, and given the assumption that the objective at this site is to find *all* TOI, and assuming that the ground truth information is reliable, the prudent approach is to *dig all anomalies*.

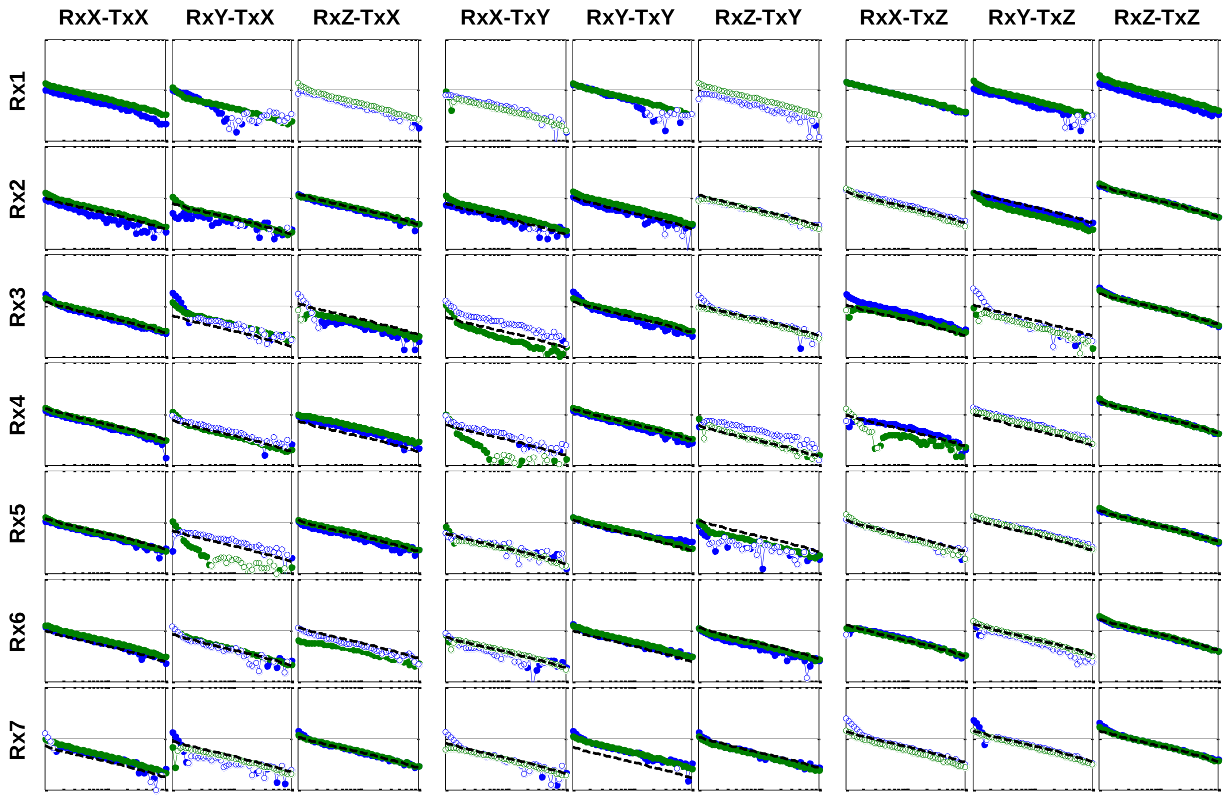

Figure 17. Data for missed QC seed WK-707 (37mm APT at 20 cm depth). Blue: observed data. Green: predicted data. Broken black line: soil model. In general all soundings are an excellent match to the soil model (so that the observed and predicted data are obscured by the black line). Receiver 1 (top row) data were generally bad for all anomalies and were not included in the inversions.

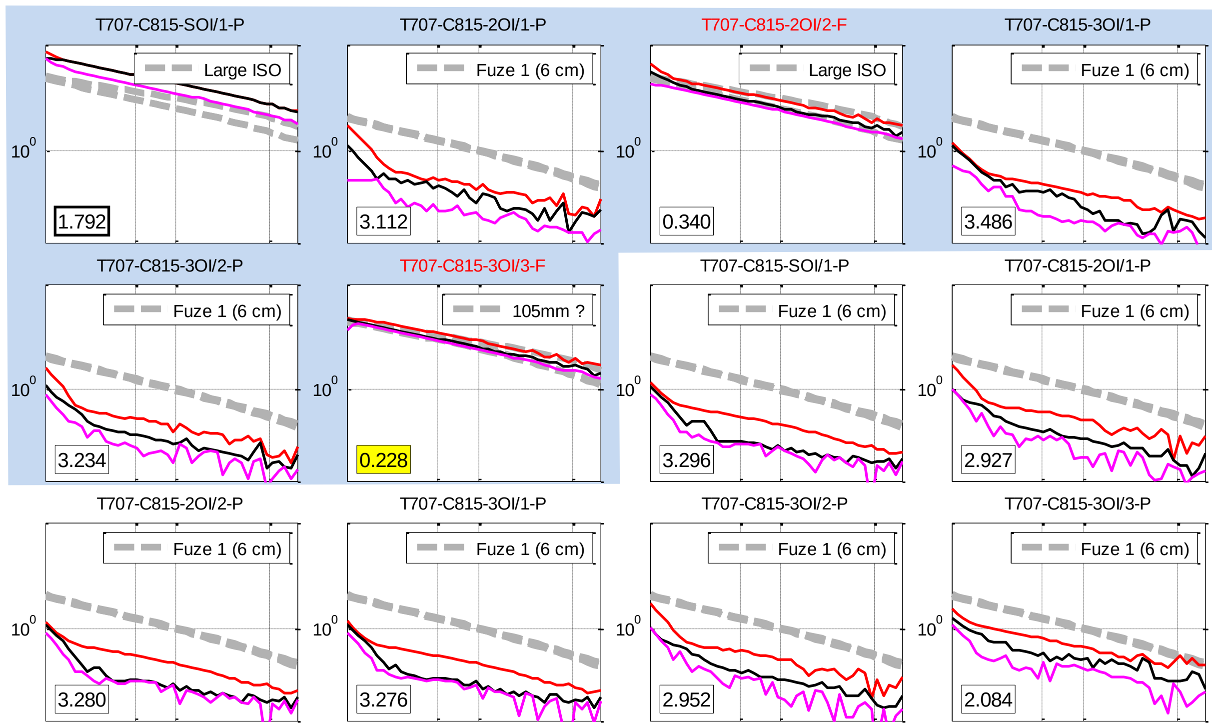

Figure 18. Polarizabilities for missed QC seed WK-707 (37mm APT at 20 cm depth). The first six models (light blue background) used data background corrected using the nearest in-air measurement and, for the two-object (2OI) and three-object (3OI) inversions, fixing one of the sources at 90 cm depth. The remaining six models used data that were corrected using the nearest near-ground background correction. Red, black and magenta lines are predicted polarizabilities. Broken grey lines are best fitting reference library polarizabilities. The predicted polarizabilities for all models are typical of a soil response. None of the models remotely resemble any of the 37mm reference items.

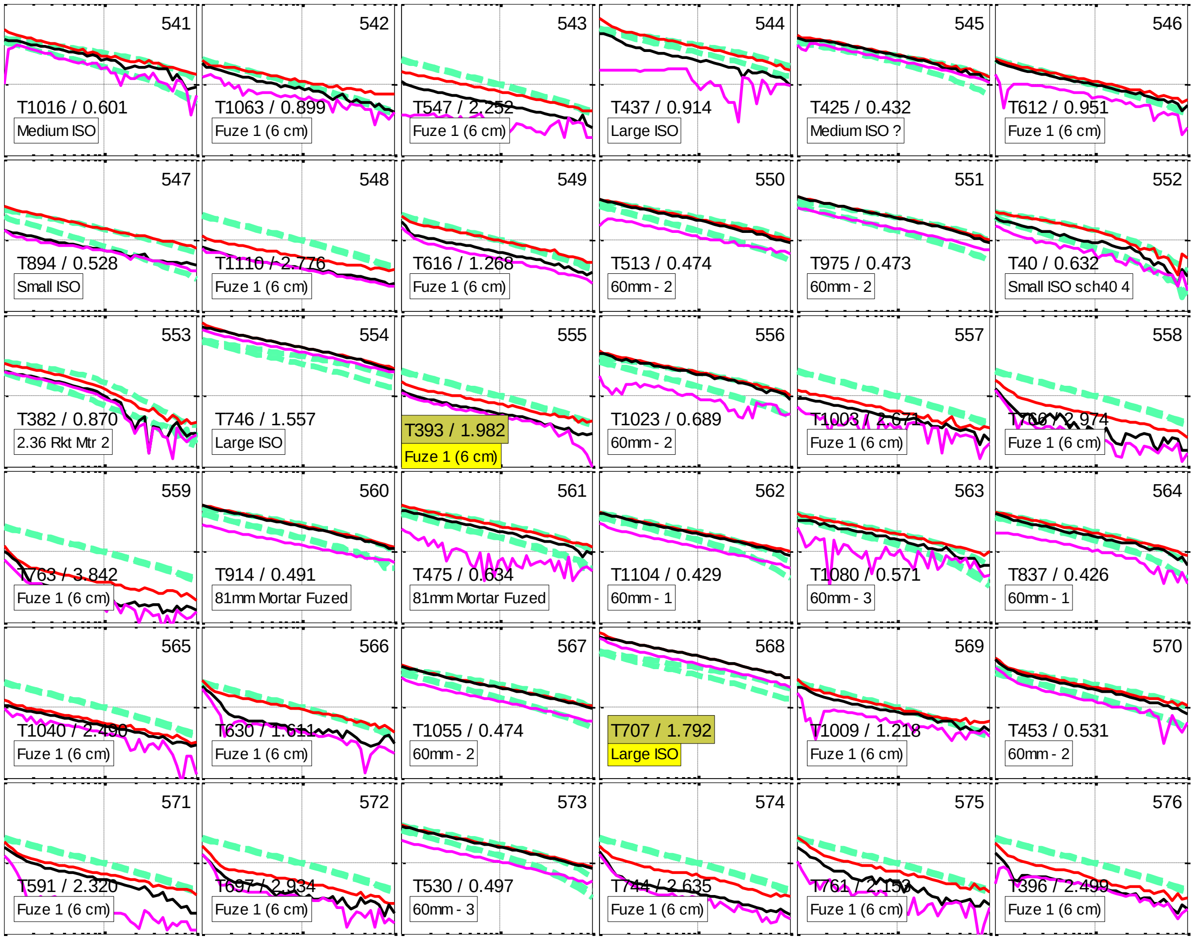

Figure 19. Polarizabilities in dig list order for digs number 541 through 576. Missed QC seeds are indicated by colored labels: WK-393 (60mm mortar; dig 555) and WK-707 (37mm; dig 568). All of the anomalies shown here have data which closely match our soil model.

c. Evidence that the modified analysis scheme correctly classifies the missed seeds and can reasonably be expected to correctly classify all remaining TOI.

Digging all anomalies will correctly classify the missed seeds and will correctly classify all remaining TOI.

Failure Memo Appendix: Data and polarizabilities for other soil-like missed QC seeds

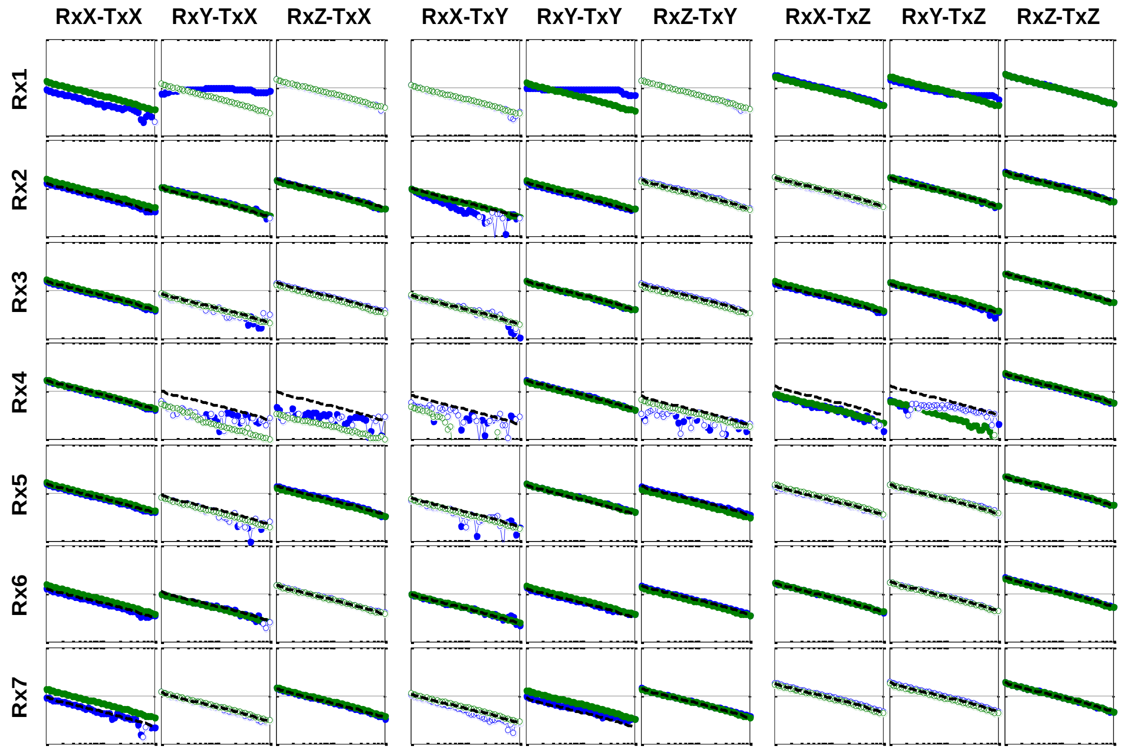

Data for missed QC seed WK-73: 37mm TP at 11 cm depth.

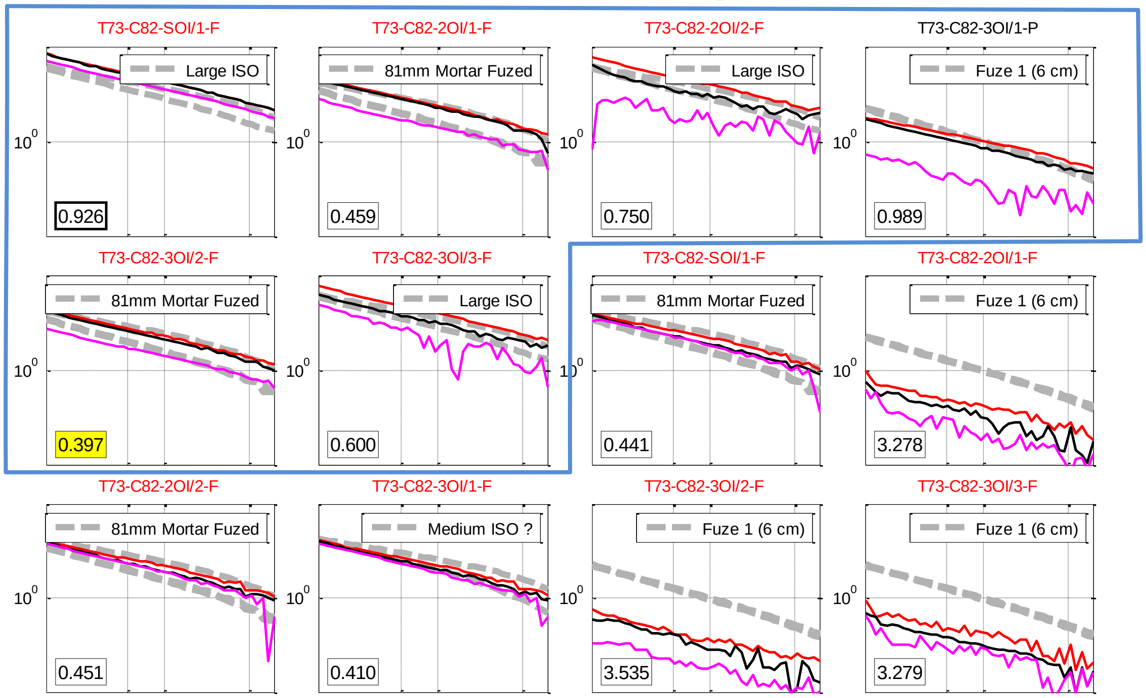

Polarizabilities for missed QC seed WK-73: 37mm TP at 11 cm depth.

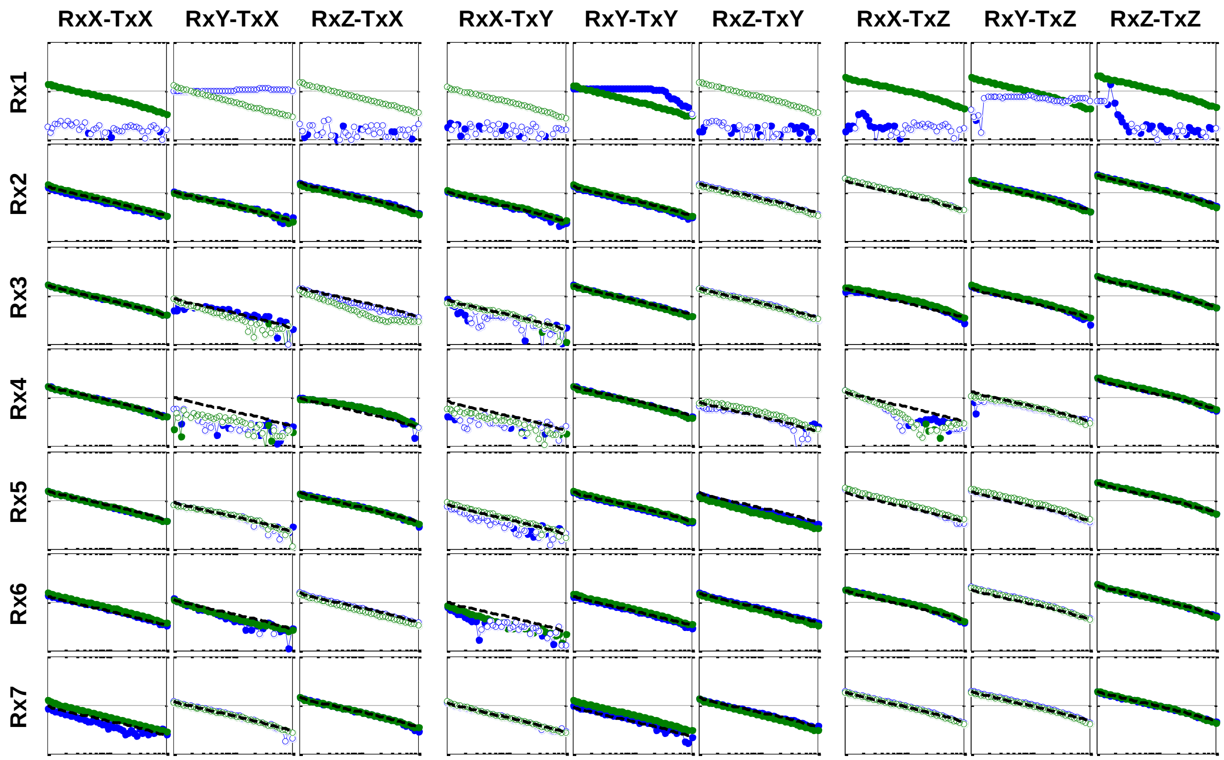

Data for missed QC seed WK-203: 60mm at 40 cm depth.

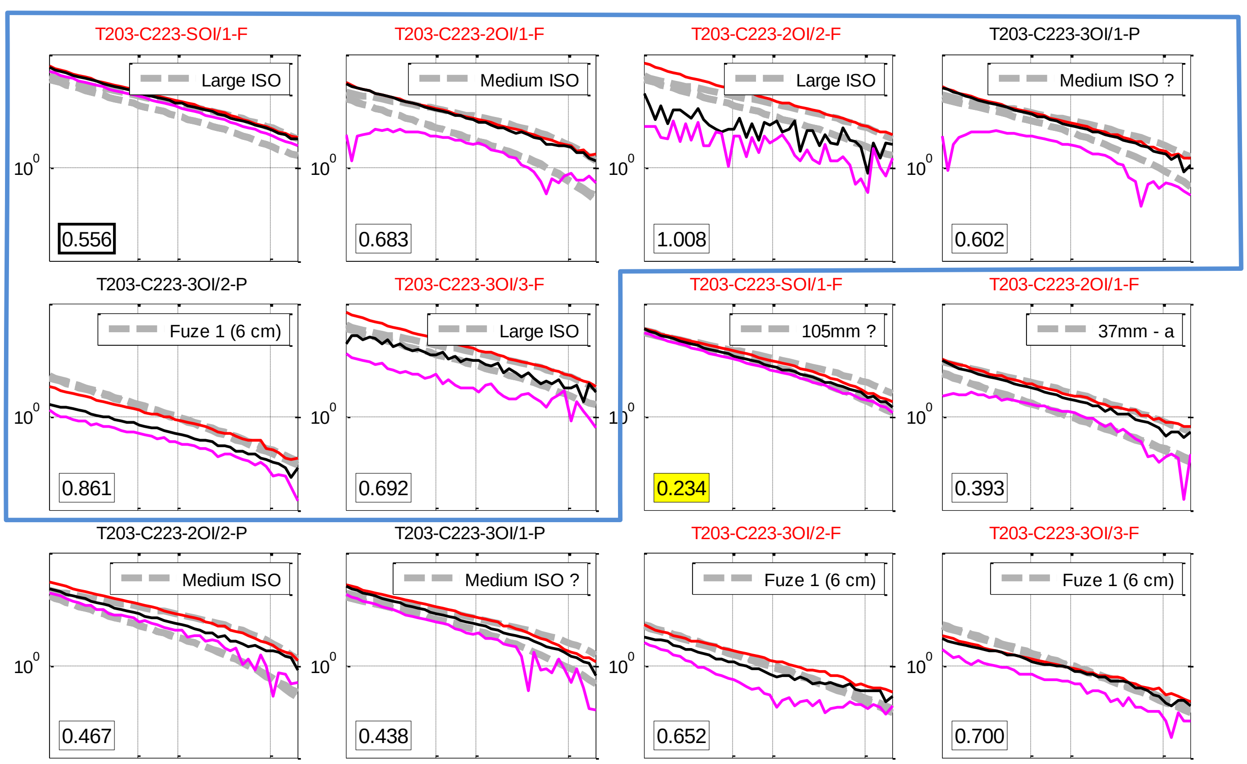

Polarizabilities for missed QC seed WK-203: 60mm at 40 cm depth.

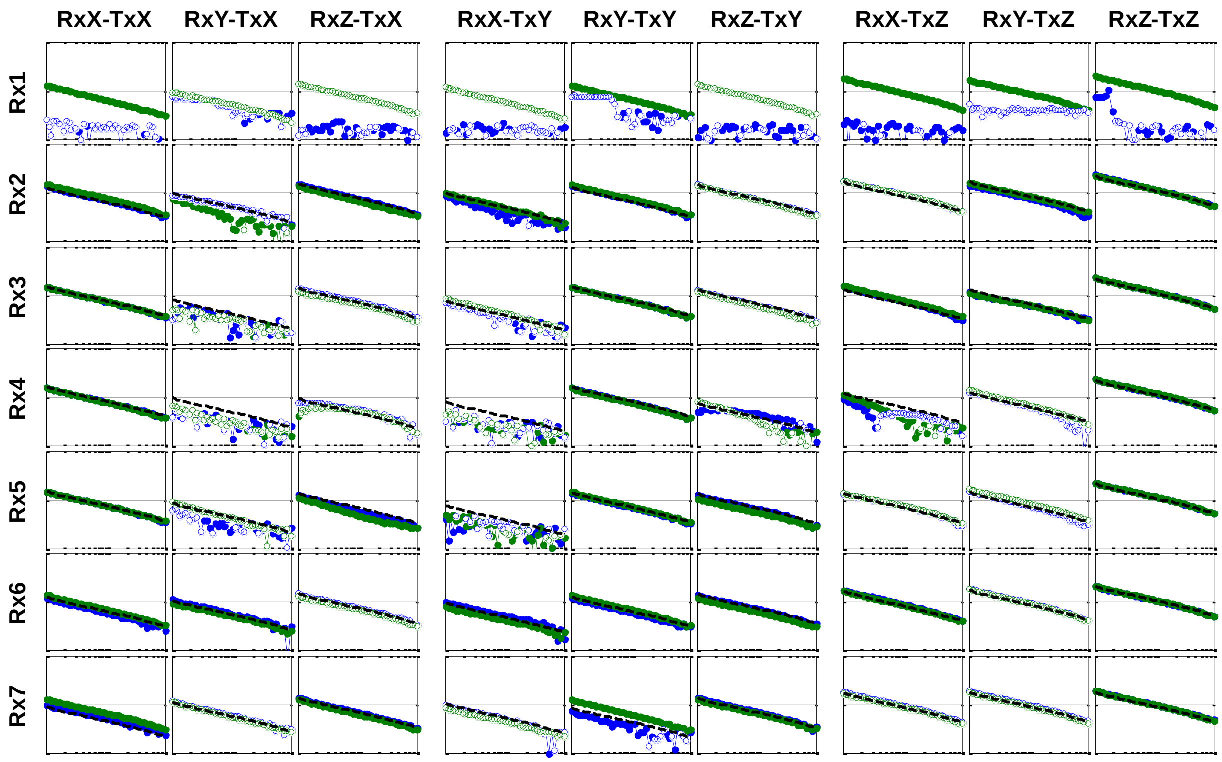

Data for missed QC seed WK-391: 60mm at 45 cm depth.

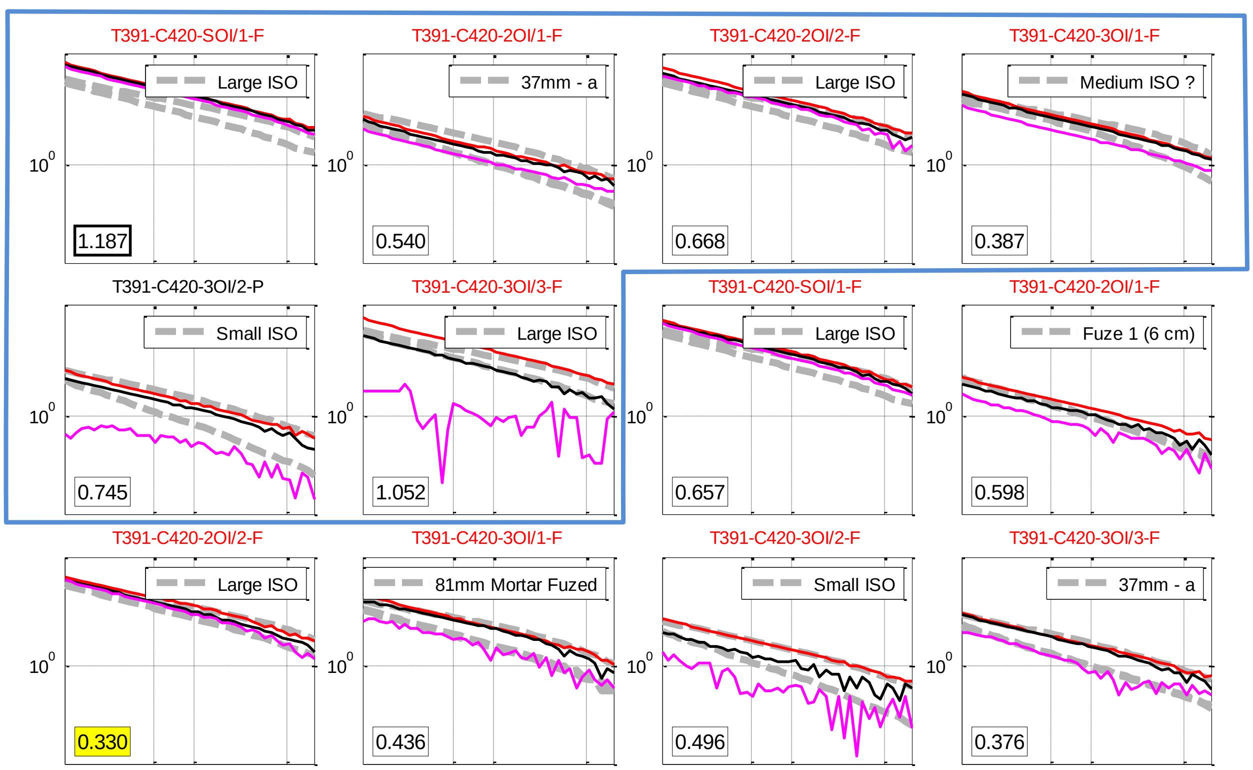

Polarizabilities for missed QC seed WK-391: 60mm at 45 cm depth.

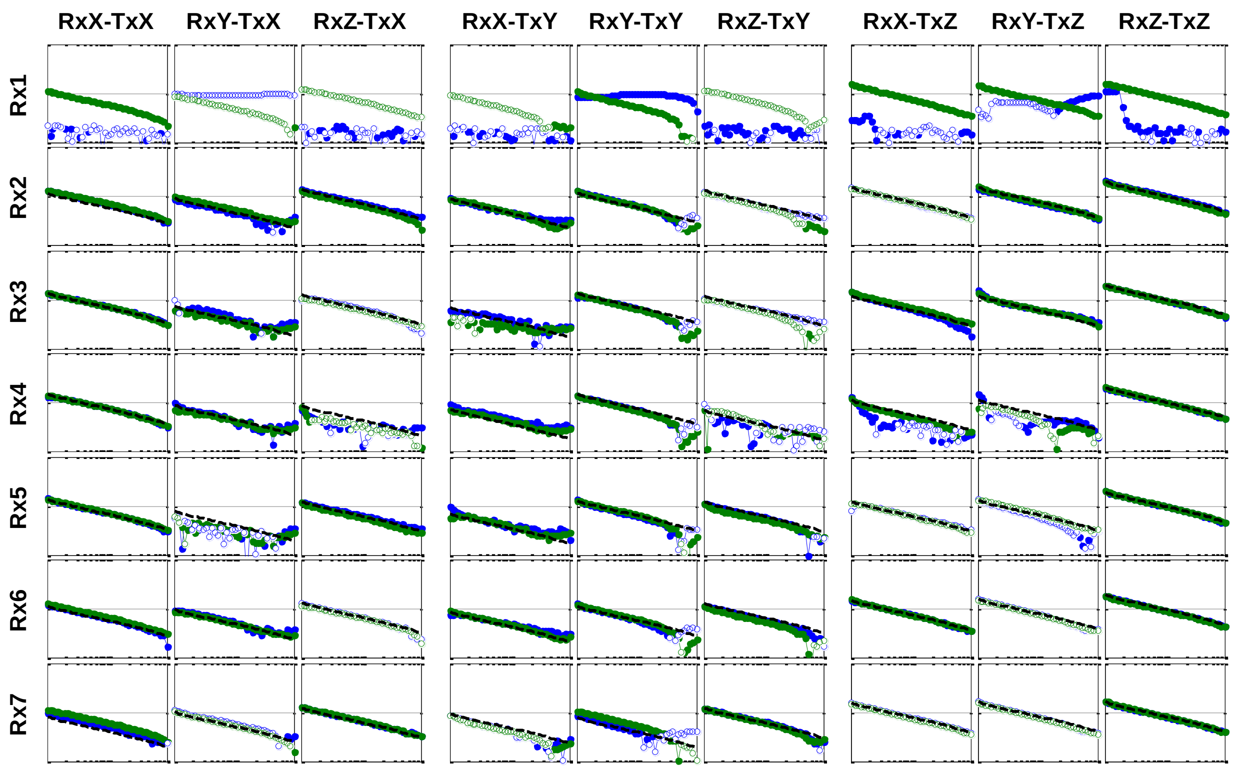

Data for missed QC seed WK-393: 60mm at 45 cm depth.

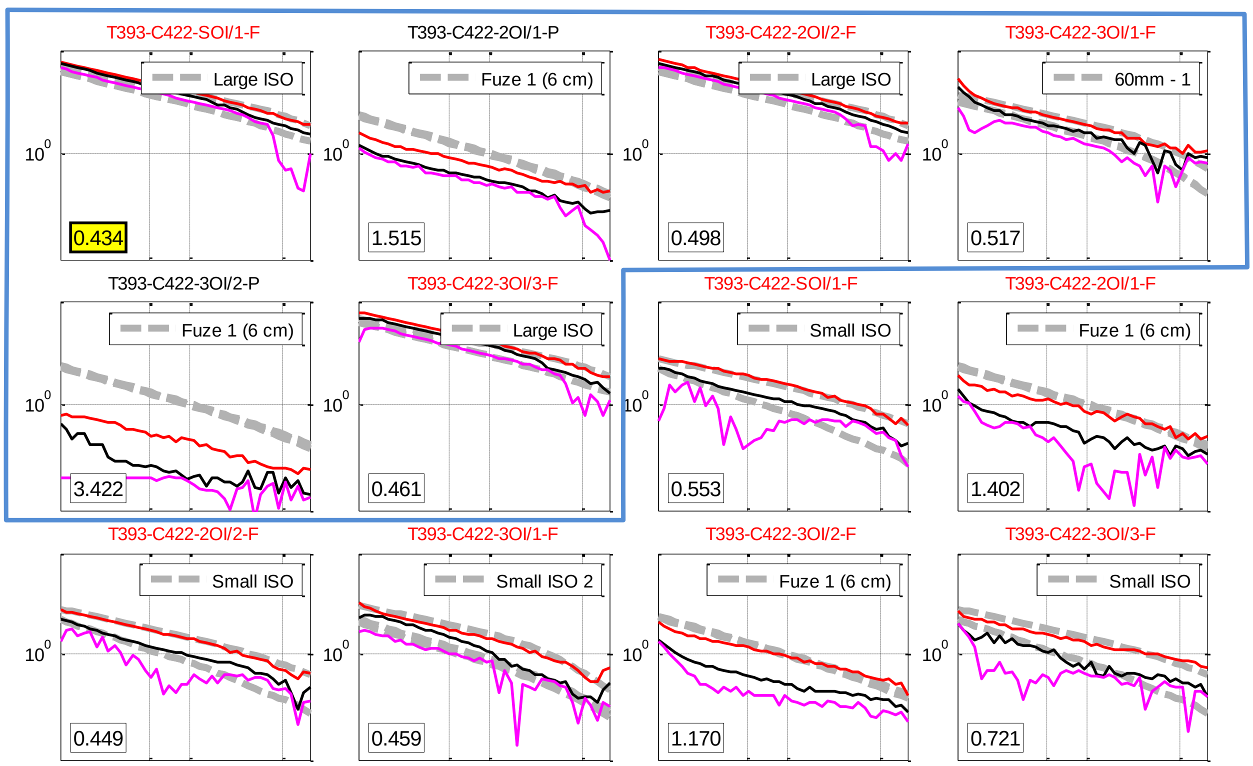

Polarizabilities for missed QC seed WK-393: 60mm at 45 cm depth.

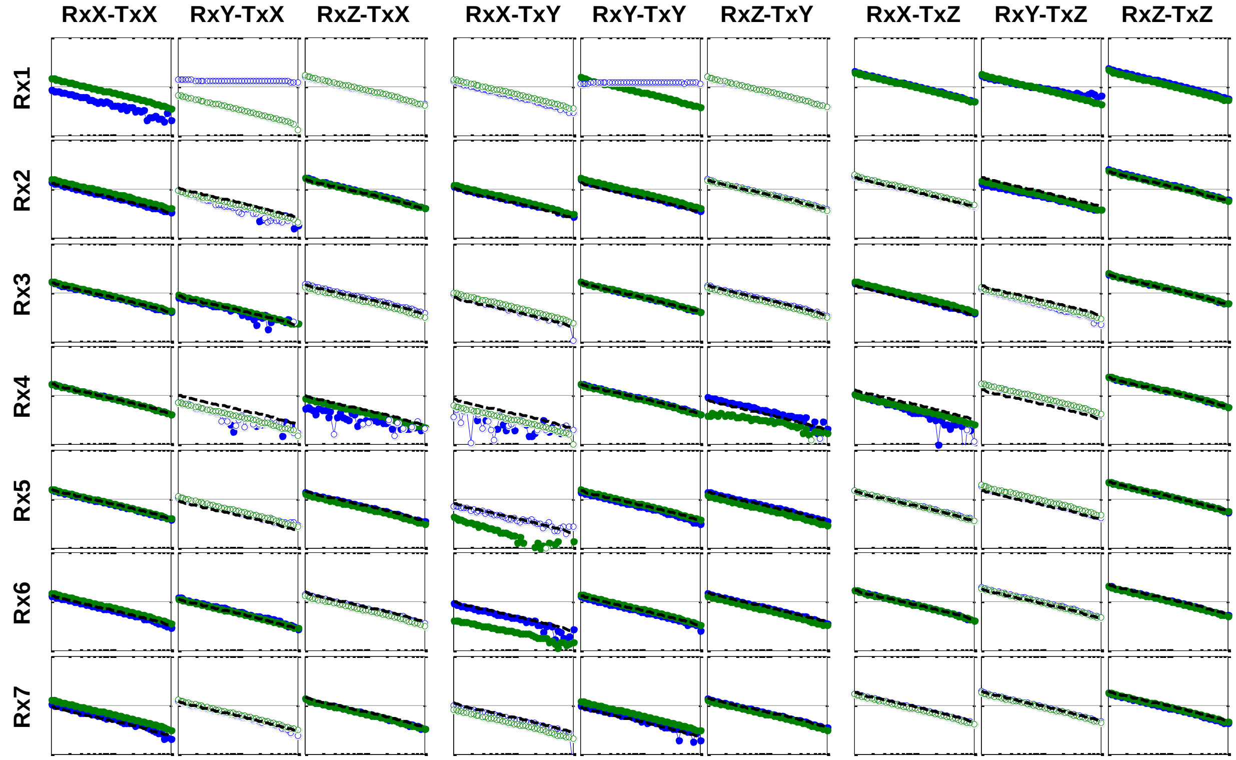

Data for missed QC seed WK-474: 60mm at 40 cm depth.

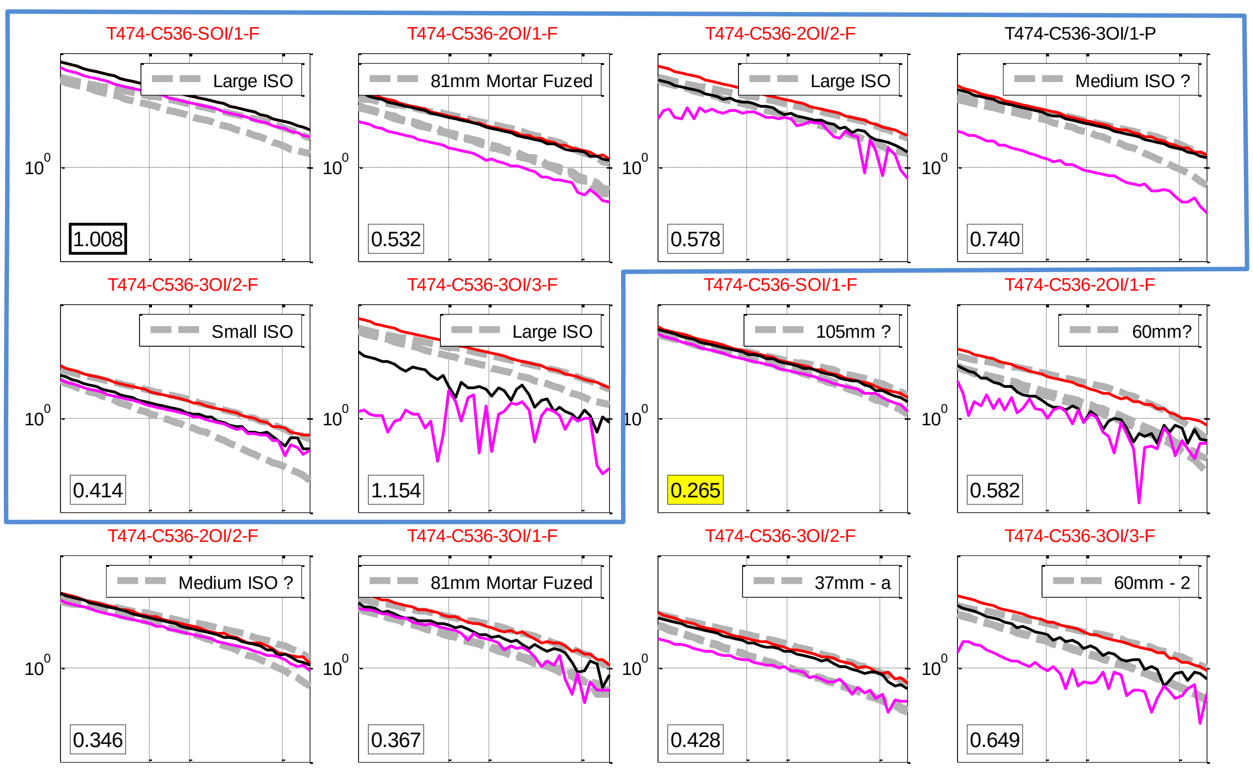

Polarizabilities for missed QC seed WK-474: 60mm at 40 cm depth.

- - - - End of Failure Analysis Memo - - - -

As described in the failure memo, based on an analysis of the missed QC seeds we decided to dig all anomalies. Figure 20 shows the final ROC curve.

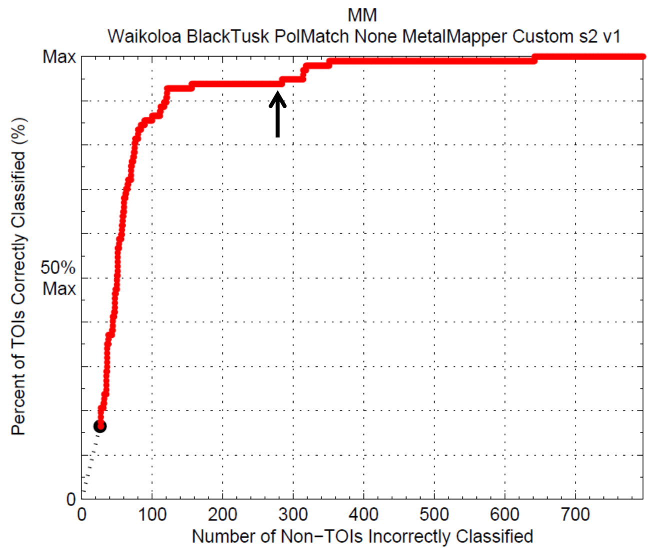

Figure 20. Final ROC curve. All anomalies were dug. Seven TOI occur late on the ROC curve (starting at the point indicated by the arrow). These anomalies are investigated in the retrospective analysis section.

3.2.3 MetalMapper cued retrospective analysis

3.2.3.1 Analysis of TOI anomalies occurring late on dig list

We take a closer look at the seven anomalies that occur late (after dig number 300) on the ROC curve (Table 2). This part of the dig list used misfit to the soil model as a classifier. Polarizabilities and other information for each of these anomalies is shown in Figure 21 to Figure 27. For two of these anomalies (WK-412 and WK-50; Figure 24 and Figure 26), there are models whose primary polarizability is a good match to that of the library polarizabilities. Unfortunately, the overall misfit (calculated using all three polarizabilities) was not low enough so that these anomalies fell within the first part of the dig list. Had we added another stage to the dig list based on matching of the primary polarizability only, we would have dug these anomalies much earlier (though perhaps at the expense of digging many more soil anomalies). For the other five late TOI anomalies, the predicted models are consistent with a soil response. For one (WK-1047; Figure 21) there is a model with a relatively close match to the expected TOI type (60mm), but closer inspection suggests that this is just a coincidence. For two of the anomalies (WK-885 and WK-14; Figure 23 and Figure 27), the location of the recovered TOI is very far (85 and 99 cm, respectively) from the center of the MetalMapper. The soil response at these two anomalies is therefore not too surprising. The large offset made correct classification of these anomalies very unlikely.

Table 2: Last seven TOI found. Soil misfit is data misfit relative to a soil model. Typically values less than ~0.6 are indicative of a strong soil response.

Anomaly	Area	Dig #	Soil misfit	Identifcation	Depth (cm)
WK-1047	TO17	401	0.62	60mm mortar	26
WK-1029	TO17	438	0.57	60mm mortar	36
WK-885	TO17	439	0.57	37mm	23
WK-412	TO20A	444	0.56	60mm mortar	37
WK-1027	TO17	481	0.55	Small ISO	11
WK-50	TO20B	498	0.54	81mm mortar	64
WK-14	TO20B	778	0.49	81mm mortar	31

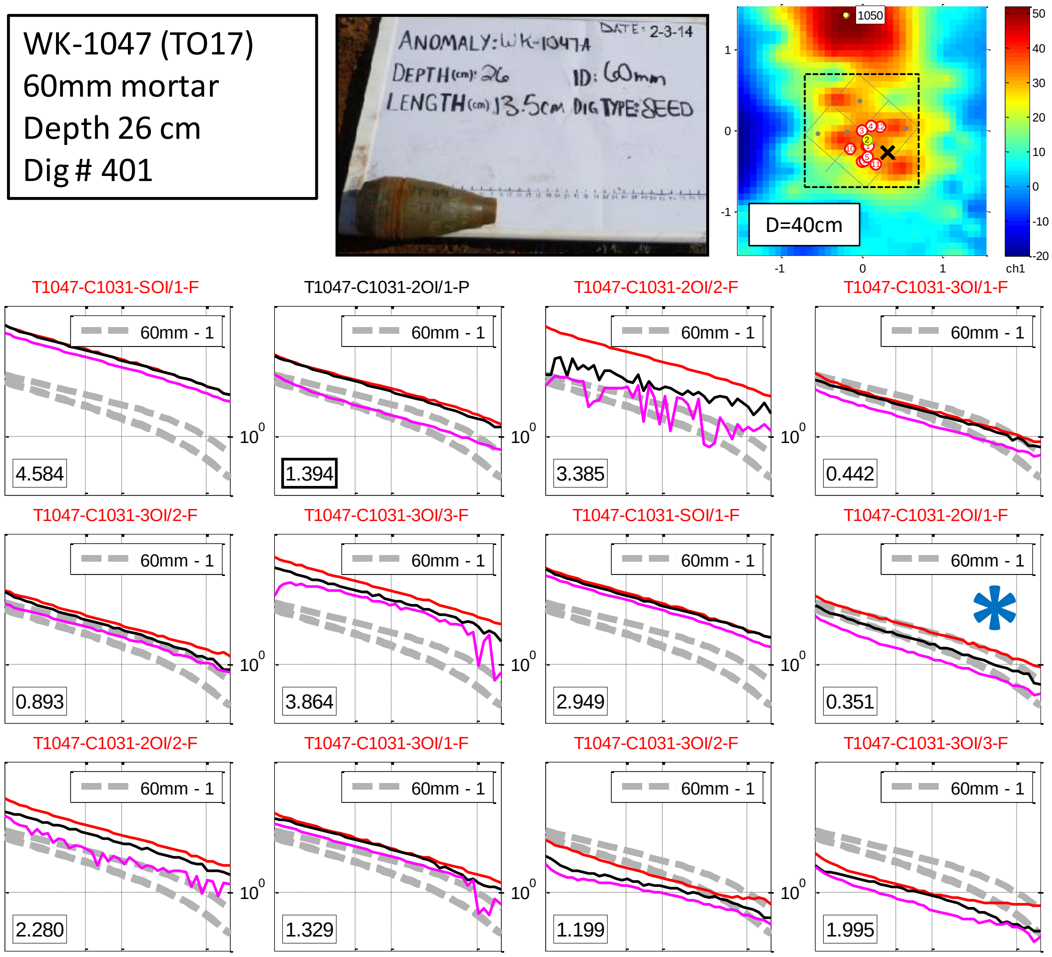

Figure 21. Polarizabilities for all models for missed TOI WK-1047. Plot at top right shows gridded EM-61 data. White and yellow circles are predicted model locations. Thin grey lines show outline of the MetalMapper. Broken black line shows extent of horizontal inversion boundaries. Black "X" shows ground truth location of TOI. Number in lower left (D) is offset from center of MetalMapper to ground truth location. Reference polarizabilities (broken grey lines) are from the library item corresponding to the actual TOI class (in this case 60mm). Blue asterisk indicates model with polarizabilities closest to those of the actual TOI class.

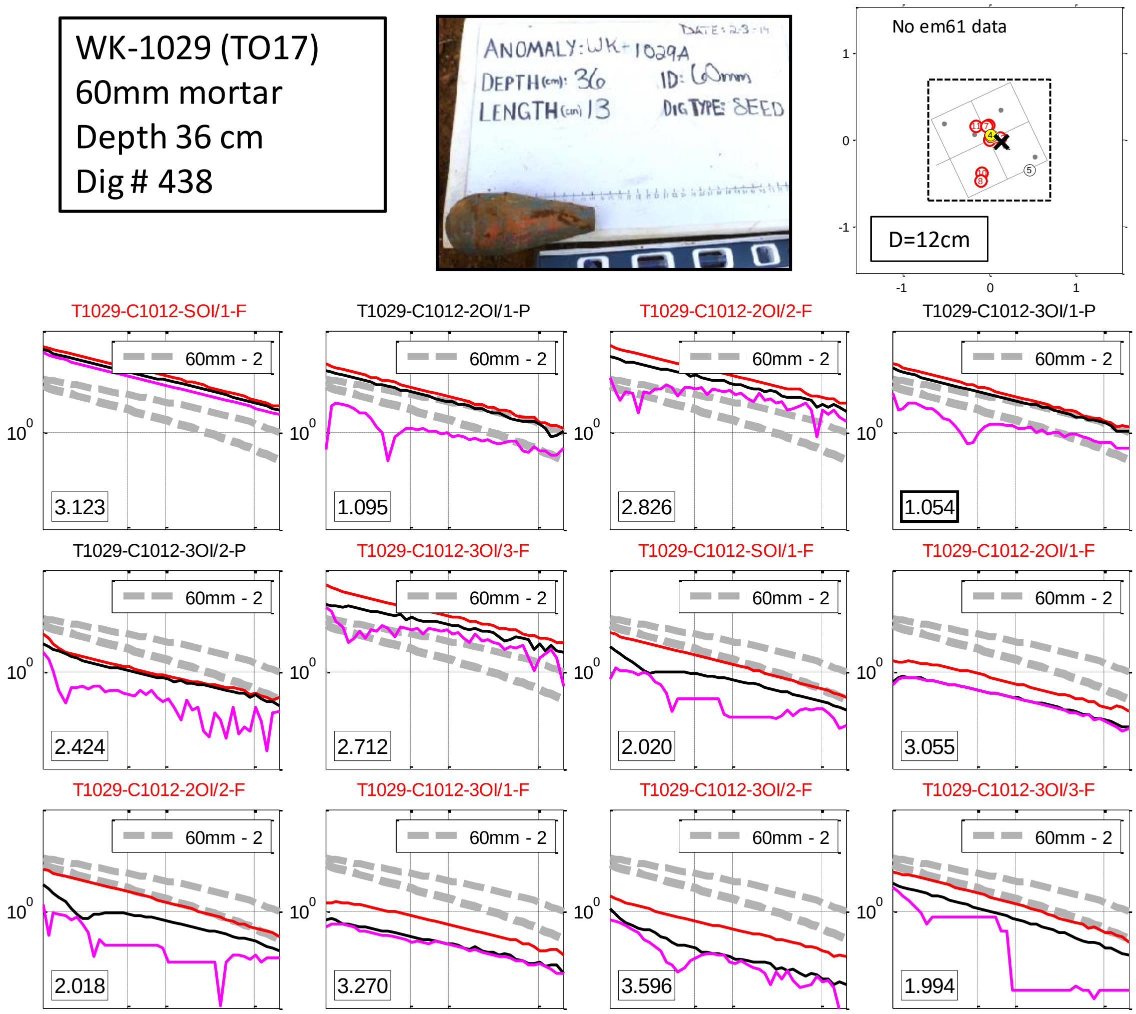

Figure 22. Polarizabilities for all models for missed TOI WK-1029. See caption for Figure 21 for other information. For this anomaly none of the models are close to matching the library polarizabilities for a 60mm. Also, for this anomaly there was no EM-61 data.

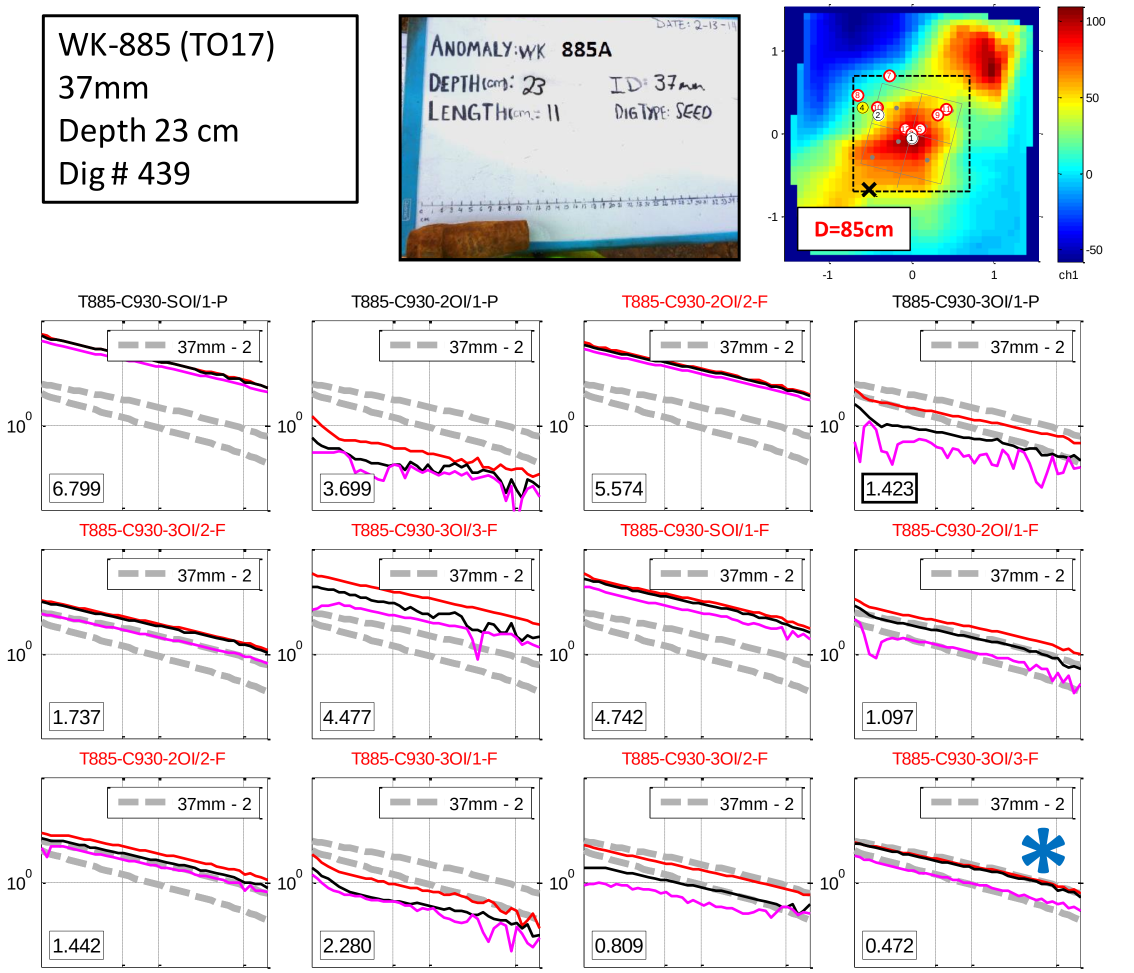

Figure 23. Polarizabilities for all models for missed TOI WK-885. See caption for Figure 21 for other information. The blue asterisk denotes a model which resembles a 37mm, but note that L1=L2 for this model. Note that the ground truth item was found a distance of 85 cm from the center of the MetalMapper.

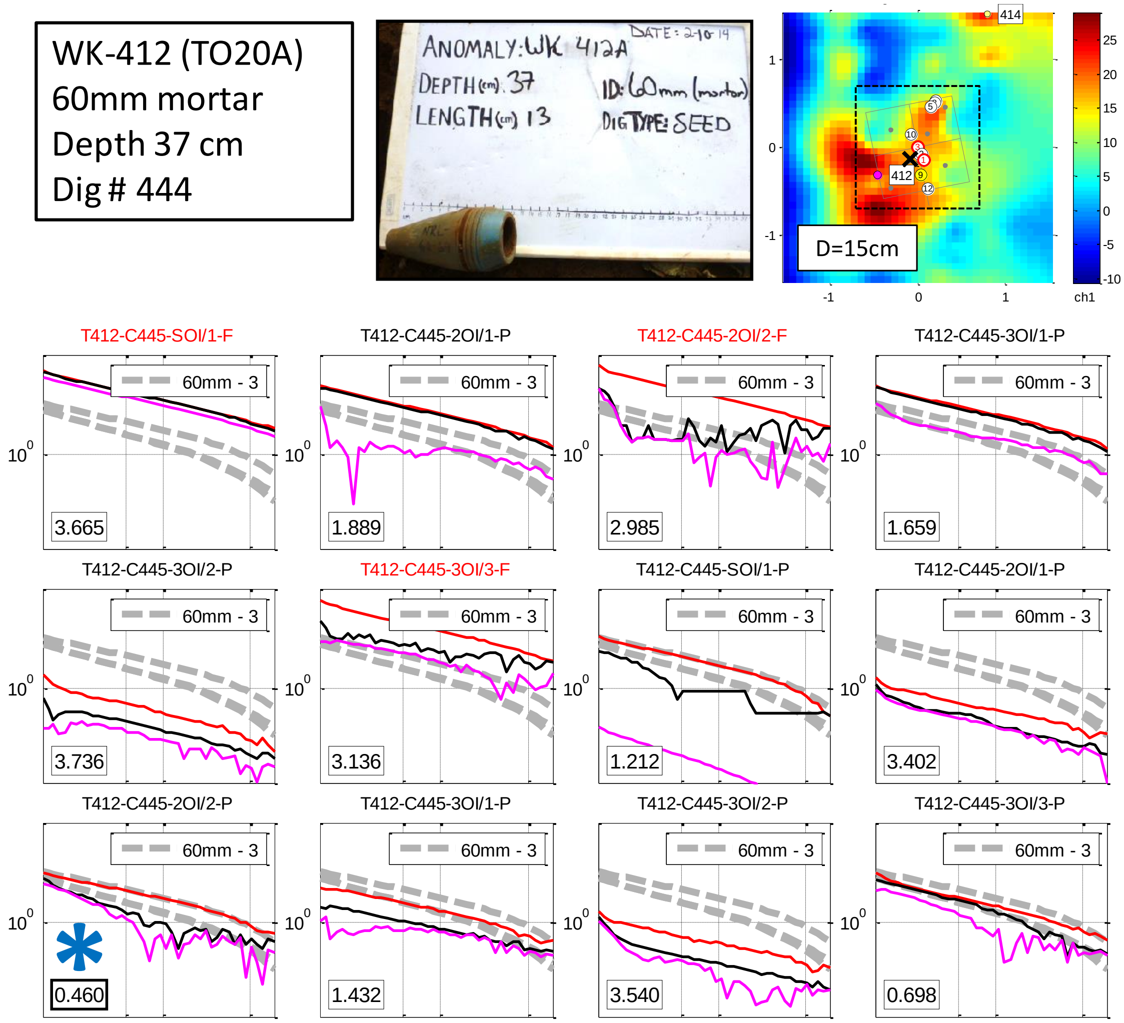

Figure 24. Polarizabilities for all models for missed TOI WK-412. See caption for Figure 21 for other information. The blue asterisk denotes a model with a good L1 match to a 60mm.

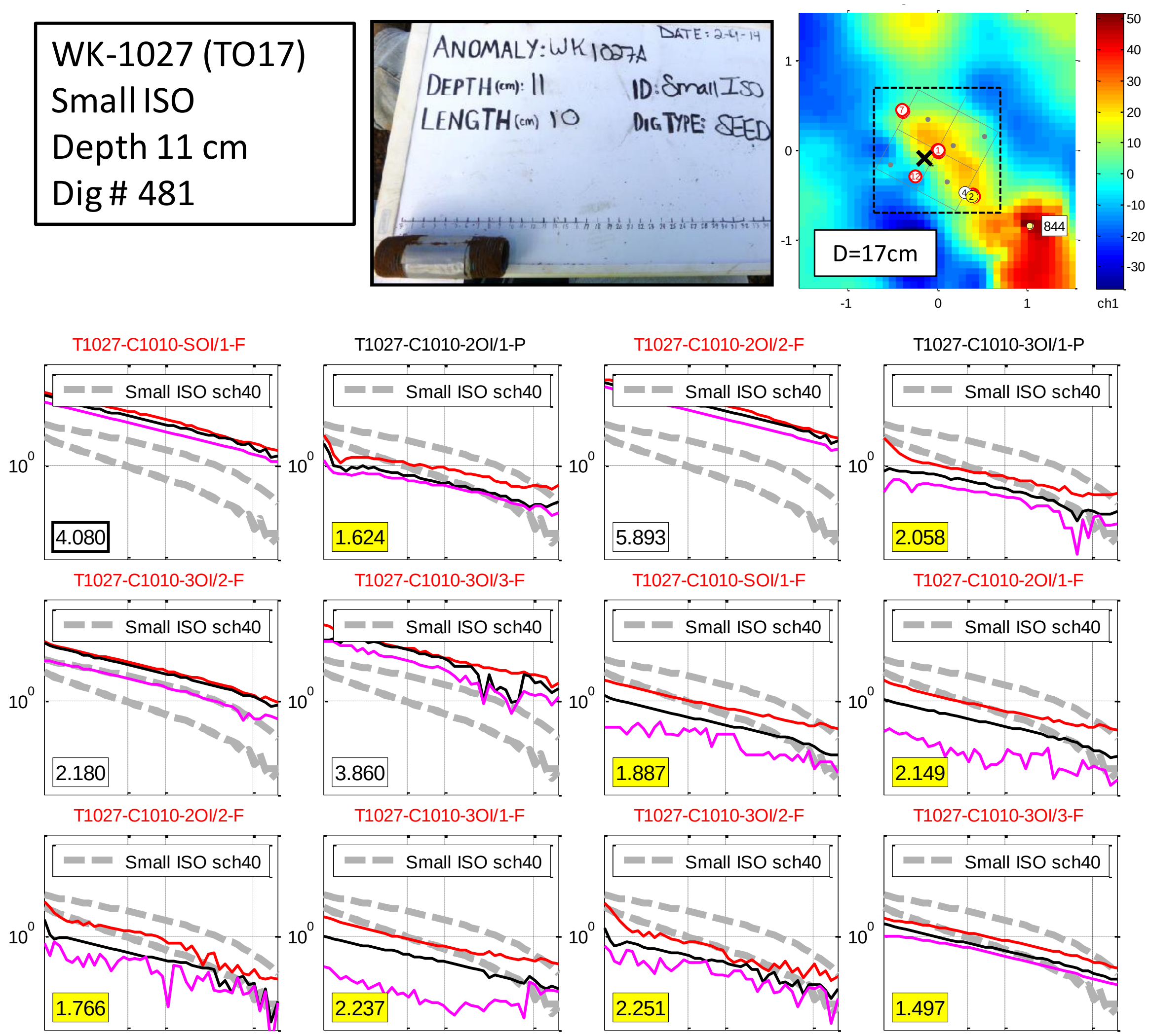

Figure 25. Polarizabilities for all models for missed TOI WK-1027. See caption for Figure 21 for other information. For this anomaly none of the models are close to matching the library polarizabilities for a small ISO.

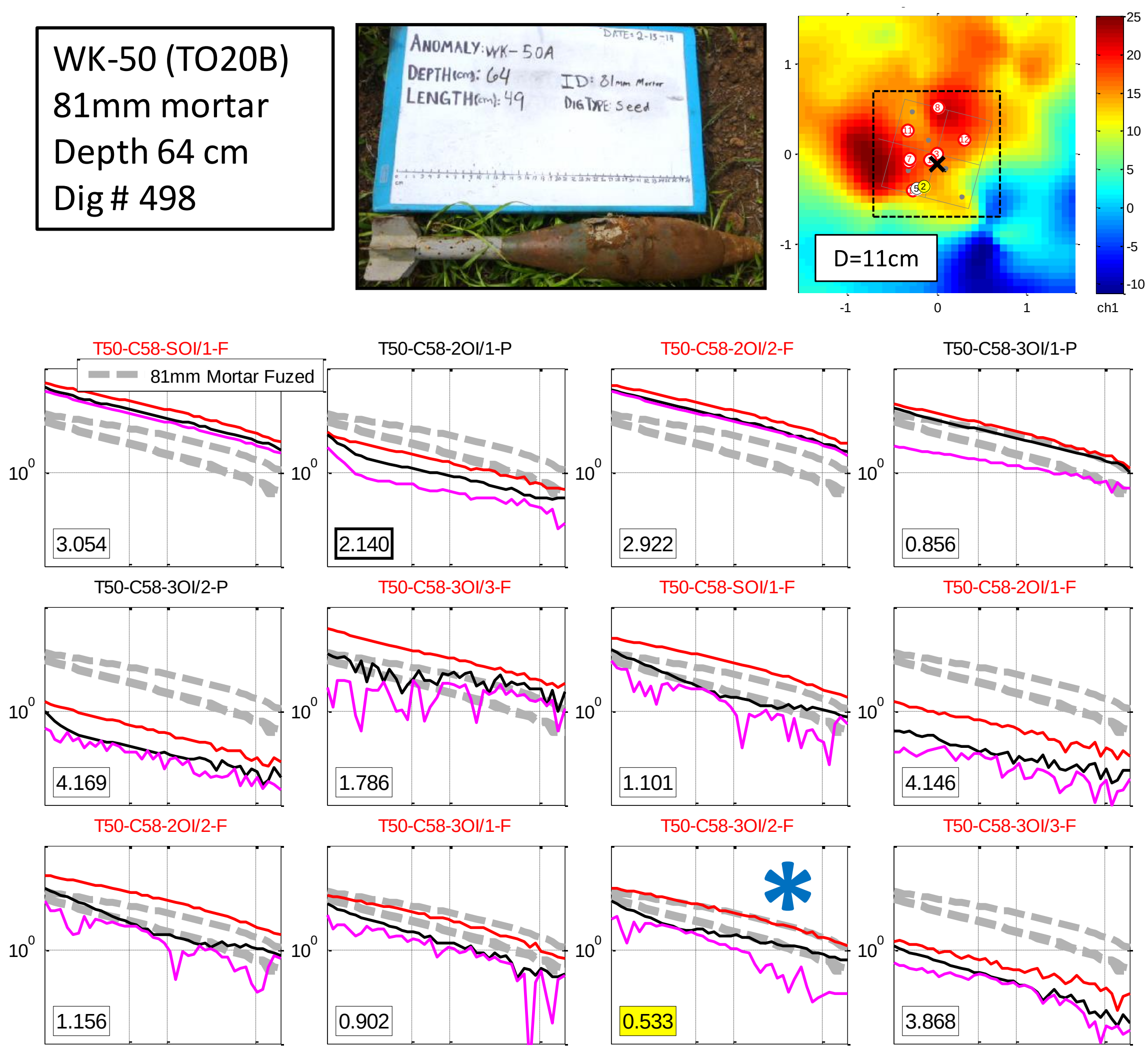

Figure 26. Polarizabilities for all models for missed TOI WK-50. See caption for Figure 21 for other information. The blue asterisk denotes a model with a good L1 match to a 81mm mortar.

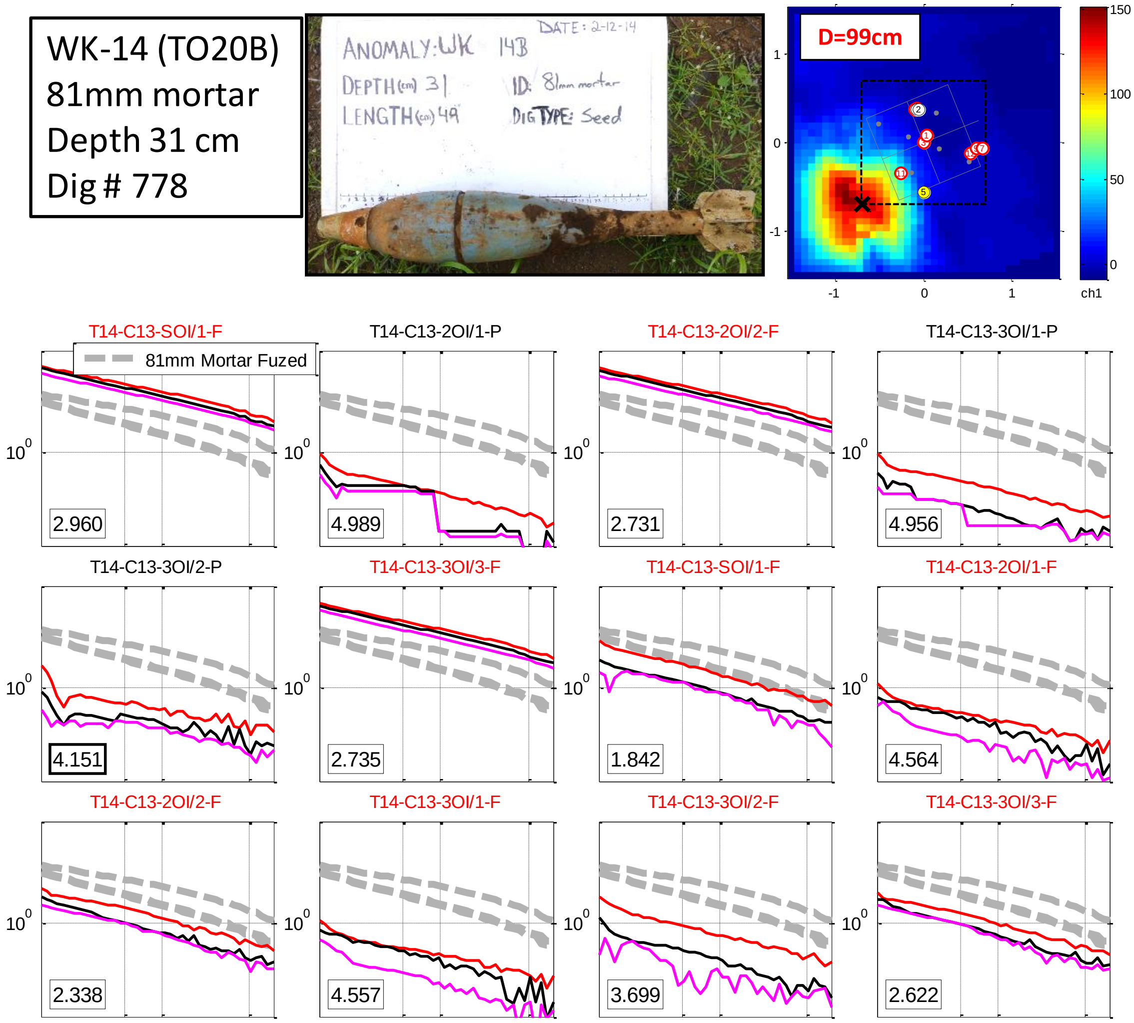

Figure 27. Polarizabilities for all models for missed TOI WK-14. See caption for Figure 21 for other information. For this anomaly none of the models are close to matching the library polarizabilities for a 81mm mortar. Note that the ground truth item was found a distance of 99 cm from the center of the MetalMapper.

3.2.3.2 Soil model misfit for TOI and actual soil anomalies

Figure 28 shows soil model misfit values for all TOI. The median soil model misfit for TOI is 0.69, significantly higher than the overall median misfit for all anomalies (0.60). Several TOI have misfit values <0.6. All of these anomalies present a challenge to classification because the data and recovered polarizabilities look typical of what is expected from a pure soil anomaly.

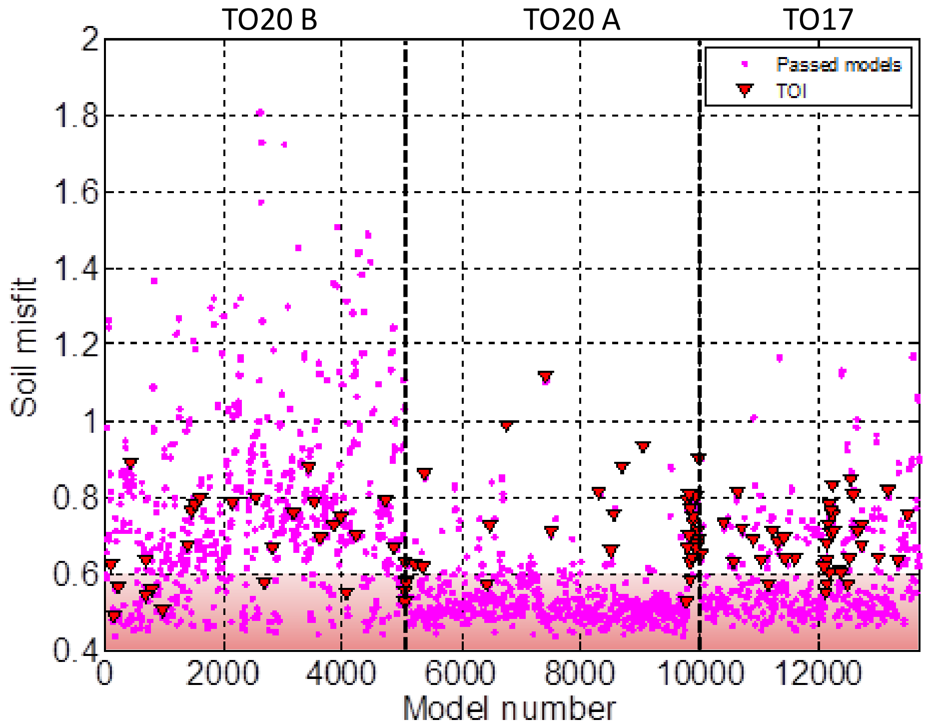

Figure 28. Soil model misfit for all models and for all TOI. Soil misfit values less than ~0.6 (red-shaded region) are typically indicative of a very strong soil response. Note that several TOI anomalies fall within this region.

In Figure 29 we plot the soil model misfit for 421 anomalies identified as soil/rock. The median misfit for these anomalies is 0.50, and almost all have a misfit <0.6. We note, however, a number of outliers, corresponding to ten unique anomalies), have misfit values >0.7. We examined these anomalies further (Figure 30 and Figure 31) and, based on the data and polarizabilities, conclude that all of these likely represent ground truth errors. Six of these anomalies, in fact, are very likely to be TOI.

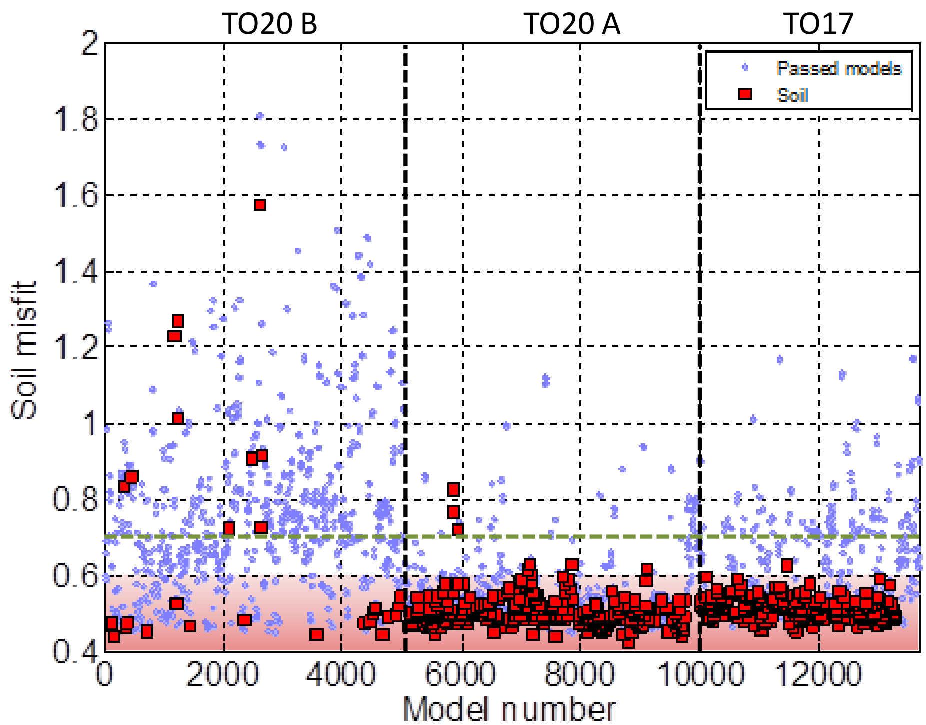

Figure 29. Soil model misfit for all models and for actual soil anomalies (according to ground truth identification). Soil misfit values less than ~0.6 (red-shaded region) are typically indicative of a very strong soil response. Note there are several outliers with values >0.7 (broken green line).

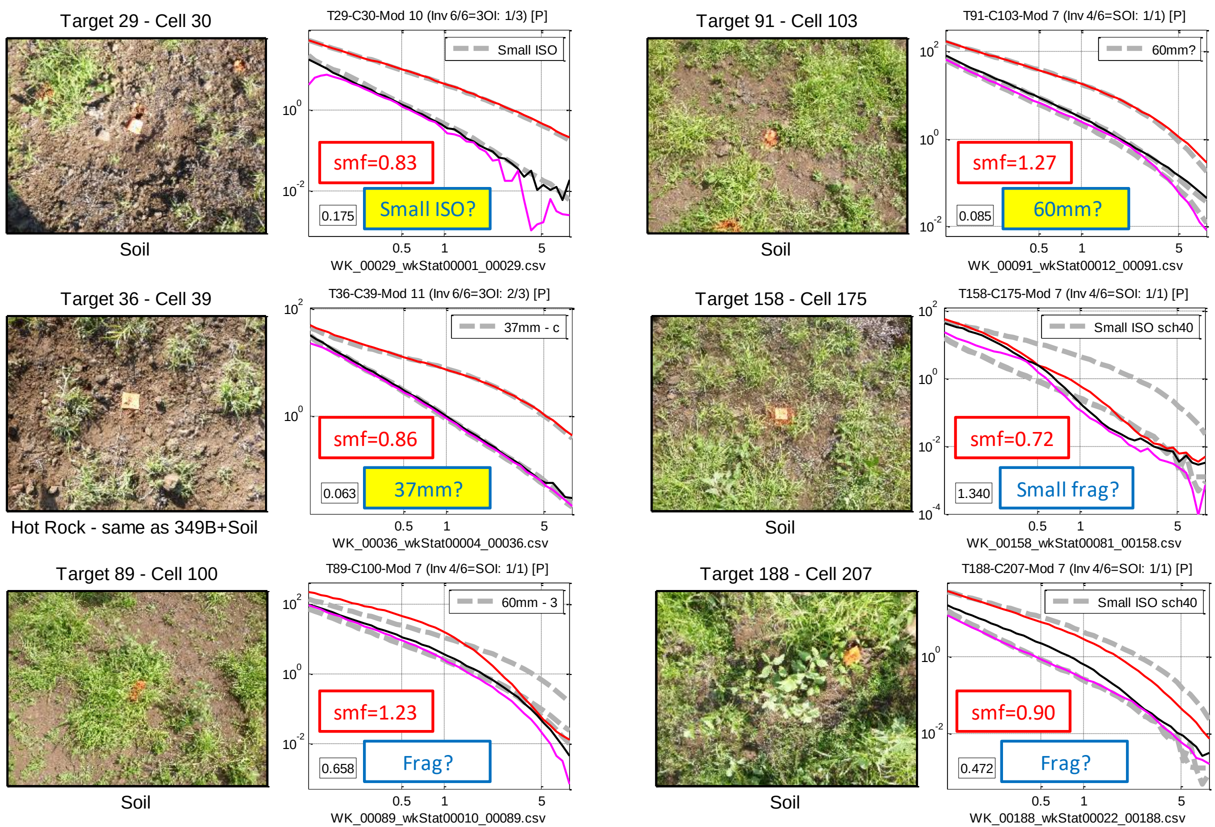

Figure 30. Polarizabilities for anomalies with ground truth identification of soil or rock but with clearly non-soil like responses and models. Three of these (WK-29, 36 and 91) very likely correspond to TOI. Label in red (smf) is soil model misfit. Label in blue is likely identification based on polarizabilities.

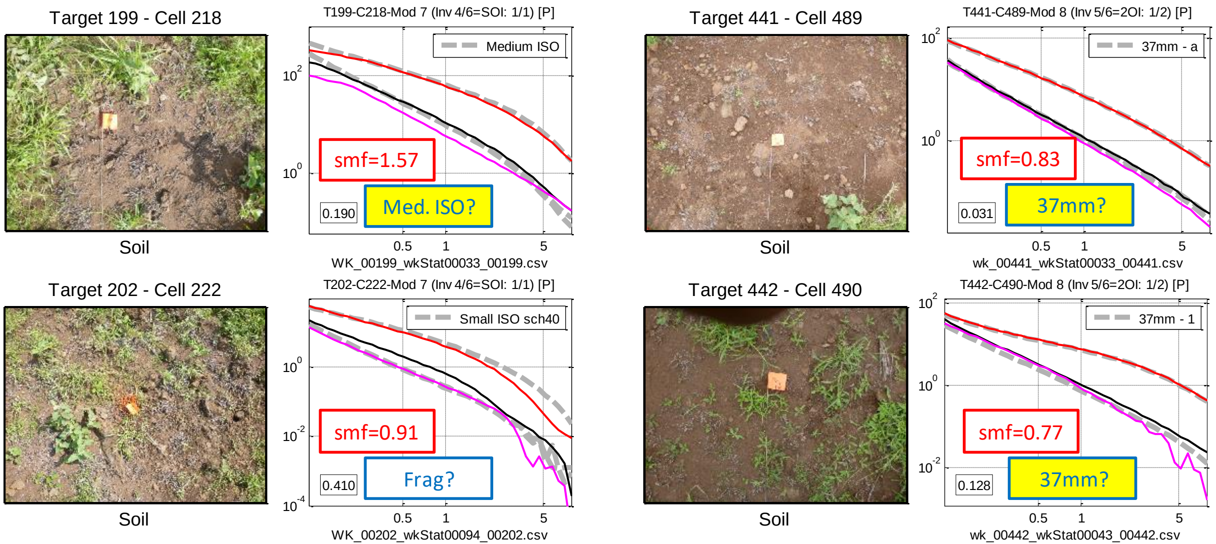

Figure 31. Polarizabilities for anomalies with ground truth identification of soil or rock but with clearly non-soil like responses and models. Three of these (WK-199, 441 and 442) very likely correspond to TOI. Label in red (smf) is soil model misfit. Label in blue is likely identification based on polarizabilities.

3.2.3.3 Small ISO consistency as measure of site difficulty

Small ISOs have been used as seed items at a number of recent Live Site demonstrations: Camp Beale (2011), Pole Mountain (2011), Spencer (2012) and Ellis (2013). The consistency of the recovered polarizabilities at each site can be viewed as a measure of the difficulty of each site for classification. Figure 32 shows the recovered polarizabilities for all small ISO anomalies at Waikoloa. The first six anomalies show reasonably good consistency (misfit values between 0.131 and 0.300); the last four anomalies are not good matches to the small ISO reference polarizabilities (misfits between 0.486 and 1.600).

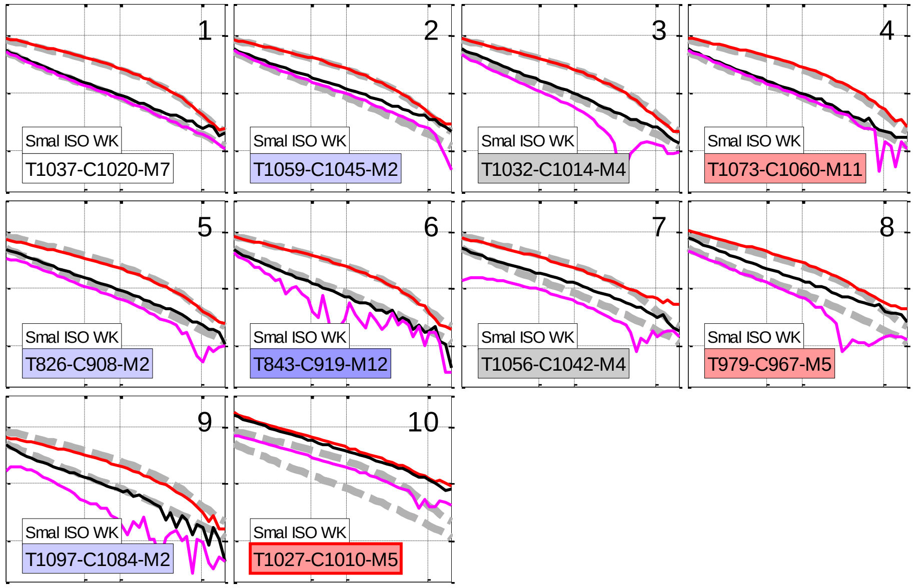

Figure 32. Polarizabilities for 10 small ISOs at Waikoloa. Colored lines are predicted polarizabilities. Broken grey lines are small ISO reference polarizabilities. Anomaly ID is the number after the "T" in each label. Polarizabilities are sorted by misfit (from best to worst) with respect to the small ISO reference model.

Figure 33 shows a compilation of the polarizabilities for small ISOs at recent Live Site demonstrations. The mean misfit values, calculated with respect to the median of the set of polarizabilities, is a good measure of site difficulty. It is clear that of the previous sites shown, Beale is the most challenging. The Beale Parsons and Beale CH2M Hill data sets comprise the same set of anomalies and the data were collected using the same MetalMapper instrument. For reasons that are not totally clear, but most likely related to differences in field practices, the Beale Parsons data resulted in more consistent ISO polarizabilities than the Beale CH2M Hill data. The excellent consistency of the Pole Mountain ISO polarizabilities reflects that site's reputation as an easy site for classification. The Spencer URS ISO polarizabilities are slightly less consistent than the those from Pole Mountain, suggesting it is a slightly more challenging site. The consistency of the polarizabilities for the Spencer dataset collected by NAEVA is marginally better than that of the URS dataset. The consistency of the Camp Ellis ISO polarizabilities actually exceeds that seen at Pole Mountain; however, note that the small ISOs used at Pole Mountain and Beale were slightly different (thinner walls) than the ISOs used at the other sites. Regardless, the consistency of the Ellis ISO polarizabilities is a good reflection of the relative ease of classification at this site. The Waikoloa small ISO dataset is small (only 10 samples) and all ISOs were located in area TO17. The large misfit value (0.155) is indicative of a very challenging site, and it is likely that the overall poor consistency of the small ISOs at Waikoloa results from the strong soil response.

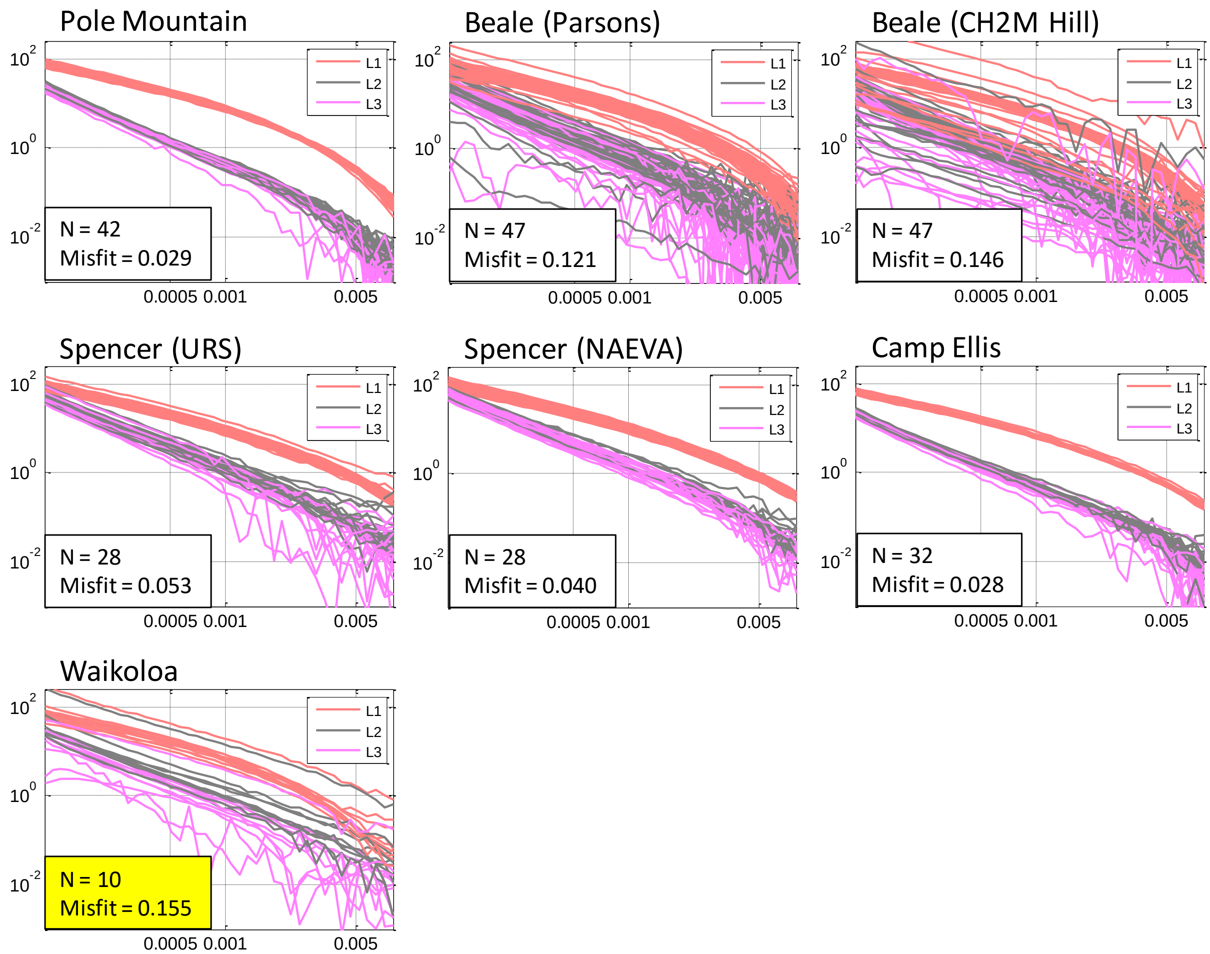

Figure 33. Compilations of polarizabilities for small ISOs from recent Live Site demonstrations. The two Beale and Spencer datasets each comprise the same set of anomalies but the data were collected by two different companies. The small ISOs used for Pole Mountain and Beale had slightly thinner walls relative to the ones used at later live site demonstrations. Misfit values are the mean misfits with respect to the median calculated over all time channels using all three polarizabilities (L1, L2 and L3).

4 Conclusions and recommendations for future work

Cued MetalMapper data collected at the Waikoloa Maneuver Area exhibited a strong background response due to the presence of ferromagnetic Hawaiian soils. Background sampling at the site was insufficient to reliably correct for this spatially variable response in the observed data.

A key recommendation from this Demonstration Report is therefore to increase the frequency and coverage of cued background measurements at sites with strongly magnetic soils. The current DAGCAP standard requires backgrounds at a minimum of every two hours, but at a site such as Waikoloa this would be inadequate. Standard operating procedures should use any available detection data to assess the variability of soil response and ensure that sufficient background measurements are collected.

Even with more and better background measurements, standard background corrections may not always fully remove a magnetic soil response. We have shown that a deep dipole source can reliably fit soil response in cued MetalMapper data. However, this approach is not appropriate for smaller moment transmitters (e.g. MPV or TEMTADS2x2) – a shallower dipole is required to fit the background, and this can impede recovery of dipole parameters for compact targets. Inversion with soil insensitive components of the data (as developed under SERDP MR-2318) is a more general approach for mitigating magnetic soil effects in EMI data.